Nano Research

Open Access

Review Article

A closed-loop nanoplatform for precision intervention in coronary atherosclerosis: Integrating multimodal omics with intelligent 3D printing

Min Gao[1,§], Yi Luo[2,§], and Rong Guo[2] ✉

[1] *Department of Nephrology, Tongren Hospital, Shanghai Jiao Tong University School of Medicine, Shanghai 200336, China*
[2] *Department of Cardiology, Yangpu Hospital, Tongji University School of Medicine, Shanghai 200090, China*
[§] *Min Gao and Yi Luo contributed equally to this work.*

Cite this article: *Nano Research*, **2026**, *19*, 94908440. https://doi.org/10.26599/NR.2026.94908440

ABSTRACT: Coronary atherosclerosis (CA) remains a leading cause of global mortality. Its progression is driven by complex immunometabolic dysregulation and marked spatial heterogeneity within atherosclerotic plaques, which together hinder the development of precise therapeutic interventions. This review proposes a nano-enabled closed-loop engineering framework for spatially precise intervention in CA. First, we systematically describe how multimodal omics technologies, including single-cell transcriptomics and spatial transcriptomics, can be leveraged to dissect plaque microenvironmental features and enable the precise identification of spatially specific therapeutic targets, such as NLR family pyrin domain-containing 3 (NLRP3) and triggering receptor expressed on myeloid cells 2 (TREM2). Building on this foundation, we focus on engineering design strategies for omics-guided nanomaterial-based intervention platforms, and comprehensively discuss stimulus-responsive nanodelivery systems (e.g., reactive oxygen species- and pH-sensitive carriers) combined with ligand modifications (e.g., intercellular adhesion molecule-1 (ICAM-1)/vascular cell adhesion molecule-1 (VCAM-1) targeting) to achieve site-specific delivery of drugs and nucleic acids to high-risk plaque regions. Furthermore, we highlight the synergistic role of three-dimensional (3D) printed biomimetic scaffolds within this framework, which provide mechanical support while enabling localized and sustained therapeutic release, thereby synergizing with nanocarriers to enhance treatment efficacy. Importantly, this review explores how artificial intelligence and digital twin technologies can integrate multi-omics data with patient-specific imaging information to guide the design of intervention platforms and the development of therapeutic strategies through predictive simulation and personalized optimization. By integrating nanotechnology, advanced manufacturing, and intelligent systems, this review delineates an engineering-driven pathway toward closed-loop, spatially adaptive, and precision intervention for CA.

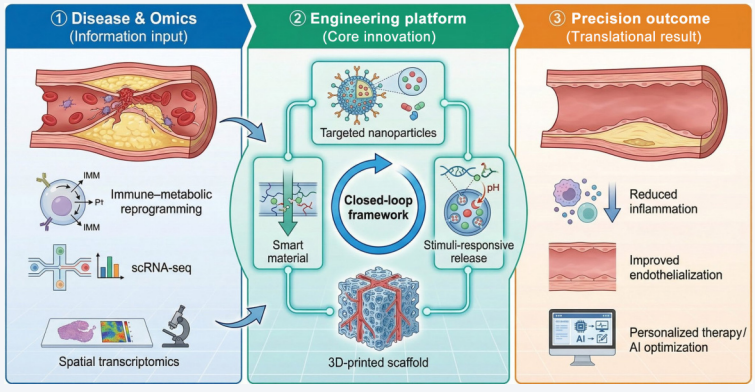

KEYWORDS: coronary atherosclerosis, immunometabolic reprogramming, multimodal omics, nanocarrier delivery, three-dimensional (3D)-printed scaffolds, artificial intelligence

1 Introduction

Despite significant advances in lipid-lowering therapies and revascularization techniques over the past decades, coronary atherosclerosis (CA) remains one of the leading causes of cardiovascular mortality and disability worldwide. According to the Global Burden of Disease Study 2022 (GBD 2022), coronary artery disease accounts for over 9 million deaths annually, and its global health burden continues to increase [1, 2]. Clinical observations indicate persistently high recurrence rates, both in patients during stable phases and following interventional procedures, highlighting the limited durability and insufficient personalization of current

Received: October 22, 2025; **Revised:** January 9, 2026
Accepted: January 13, 2026

✉Address correspondence to 09_doctorguo@tongji.edu.cn

therapeutic strategies, as well as their inability to adequately address lesion heterogeneity [3].

Accumulating basic and translational studies have revealed that CA progression is not driven solely by lipid deposition but rather results from intricate interactions between immune-inflammatory responses and metabolic reprogramming [4–6]. Investigations in animal models and human atherosclerotic tissues have identified several convergent pathogenic pathways, including activation of the NLR family pyrin domain-containing 3 (NLRP3) inflammasome, hypoxia-inducible factor 1-alpha (HIF-1α) signaling, and nuclear factor kappa-light-chain-enhancer of activated B cells (NF-κB)-driven chronic inflammation. These processes are tightly coupled with metabolic disturbances such as enhanced glycolytic flux, impaired cholesterol efflux, and increased vulnerability to ferroptosis, collectively promoting plaque initiation, progression, and destabilization [7]. Concurrently, clinical research in CA is undergoing a paradigm shift from a singular emphasis on lipid lowering toward more refined risk stratification and earlier, more intensive combination interventions. While early achievement and long-term maintenance of low-density lipoprotein cholesterol (LDL-C) targets remain central therapeutic goals, driving the application of individualized combination therapeutic regimens in high-risk populations. Growing attention is being directed toward residual inflammatory risk, metabolic comorbidities, and plaque-specific features that contribute to disease progression. Advances in imaging and functional assessment reflect this shift, moving beyond the evaluation of luminal stenosis alone toward integrated characterization of plaque burden, fibrous cap integrity, inflammatory activity, and vulnerability signatures. Together, these developments provide a more actionable clinical framework for addressing inter-individual heterogeneity, recognizing that patients sharing a diagnosis of CA may require markedly different therapeutic intensities and management strategies.

However, despite substantial advances in mechanistic understanding, translating these insights into precision intervention strategies remains a major challenge. Conventional tissue-level approaches are insufficient to resolve the cellular heterogeneity and spatial complexity within atherosclerotic plaques. Recent spatial omics studies have revealed significant regional differences in macrophage subpopulations, T-cell infiltration patterns, and their associated metabolic states across distinct plaque microenvironments [8, 9]. Moreover, integrative multi-omics analyses have identified novel therapeutic targets, such as the fibroblast-immune cell interaction axis [10, 11].

Meanwhile, advances in nanomaterials and three-dimensional (3D) printing-based engineering platforms are providing new opportunities for therapeutic intervention in CA [12–14]. Nanocarriers such as liposomes, peptide-functionalized polymers, and biomimetic membrane-coated nanoparticles enable selective delivery to plaque-associated molecular markers. When combined with pH- or reactive oxygen species (ROS)-responsive systems, these systems allow spatially confined and precisely regulated therapeutic modulation. Additionally, 3D-printed personalized scaffolds, constructed based on imaging-derived anatomical models, can replicate vascular structures while simultaneously providing mechanical support and immunomodulatory functions [15].

More cutting-edge developments involve integrating artificial intelligence (AI) and digital twin systems into the design of CA interventions. These technologies assimilate multimodal omics, imaging, and hemodynamic data to generate individualized predictive models and simulate intervention outcomes [16]. This interdisciplinary convergence provides a foundation for closed-loop intervention workflows that encompass patient feature recognition, target identification, intervention design, and efficacy prediction.

Against this backdrop, the present review follows a mechanism-focused and strategy-oriented framework to systematically examine five key aspects: (1) immunometabolic reprogramming mechanisms in CA; (2) the application of multimodal omics to decode lesion heterogeneity; (3) omics-guided target discovery pipelines; (4) the design and implementation of engineering platforms integrating nanomaterials and 3D printing technologies; and (5) AI-enabled intelligent intervention systems and their translational potential (Fig. 1).

2 Mechanisms of immunometabolic reprogramming in CA

2.1 Immune cell networks within atherosclerotic plaques and functionally intervenable subpopulations

Before discussing immunometabolic reprogramming, it is necessary to define immune cell heterogeneity within atherosclerotic plaques from a functional and intervention-oriented perspective, rather than providing an exhaustive catalog of phenotypic subsets. Previous studies have identified lipid-laden, tumor-associated macrophage (TAM)-like macrophages within plaques, which exhibit a "dual phenotype" characterized by enhanced phagocytic activity alongside upregulated pro-inflammatory signaling, and are closely associated with plaque progression [17, 18]. More importantly, this cellular state displays substantial plasticity, suggesting that plaque-resident immune cells do not represent static terminal states but instead constitute dynamically reprogrammable targets for intervention. This concept provides a critical theoretical foundation for spatiotemporally precise immunomodulatory strategies [5].

In the context of adaptive immunity, regulatory T cells (Tregs) and T helper 17 (Th17) cells exert opposing regulatory effects on plaque immune homeostasis. Unstable plaques are commonly characterized by a reduction in Treg populations accompanied by increased Th17 infiltration, leading to amplified inflammation and disease progression [19]. Consequently, the relative abundance and spatial organization of immune subpopulations represent not only mechanistic features of plaque pathology but also define actionable immunological axes for intervention. Prioritizing immune subsets that are both functionally dominant and accessible to targeted modulation offers a more operationally tractable framework for therapeutic development. This approach directly informs the rational design of nanotechnology-based delivery systems and scaffold-guided immunoregulatory strategies, thereby bridging mechanistic understanding with engineering-driven therapeutic implementation.

2.2 Metabolic dysregulation as a functionally intervenable axis in CA

Metabolic reprogramming is one of the central drivers of CA progression and represents a process with clear functional tractability for therapeutic intervention. Pro-inflammatory macrophages within atherosclerotic plaques preferentially rely on aerobic glycolysis for energy production, whereas anti-

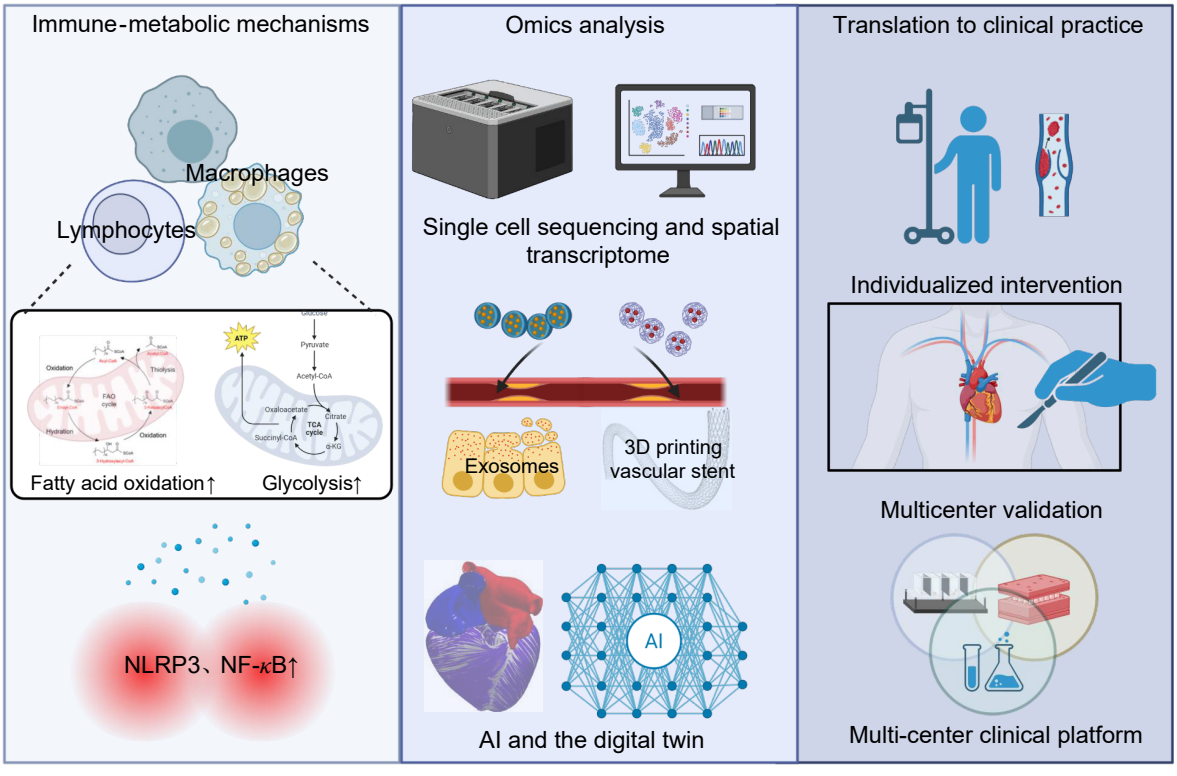

Figure 1 Closed-loop pathway from immuno-metabolic mechanisms to clinical translation in CA. The figure illustrates the complete pathway from the elucidation of immuno-metabolic mechanisms—including macrophages, T cells, NLRP3 inflammasomes, HIF-1α, and NF-κB signaling—to target identification and the development of engineered intervention platforms (nanoparticles, 3D-printed scaffolds), followed by optimization through AI and digital twin models, ultimately enabling clinical translation (multicenter validation and individualized intervention). The bottom of the figure highlights key challenges such as high recurrence rates, interindividual variability, and immuno-metabolic heterogeneity, underscoring the importance of interdisciplinary integration and the future potential of precision cardiovascular interventions.

inflammatory or reparative phenotypes are more dependent on oxidative phosphorylation and fatty acid oxidation. This metabolic preference is tightly coupled to their effector functions [20, 21]. In parallel, dysregulated cholesterol metabolism spans the entire course of plaque formation and inflammatory propagation. The accumulation of oxidized low-density lipoprotein (oxLDL) and oxidized cholesterol within the arterial wall promotes foam cell formation and amplifies local inflammatory responses [4, 22].

In recent years, ferroptosis, a metabolically regulated form of cell death, has been demonstrated to be directly associated with plaque instability. The coupling of iron overload and lipid peroxidation can induce ferroptosis in both macrophages and vascular smooth muscle cells (VSMCs), thereby driving necrotic core expansion and compromising fibrous cap integrity [23, 24]. Collectively, enhanced glycolysis, impaired cholesterol handling, and lipid peroxidation/ferroptosis constitute interconnected metabolic axes that are highly coupled to immune activation and plaque vulnerability. From a translational and engineering-oriented perspective, prioritizing these dominant and often spatially restricted metabolic processes provides a rational basis for the design of nano-enabled platforms and scaffold systems with "sensing-and-response" capabilities. Such systems hold promise for achieving spatiotemporal reprogramming of plaque metabolism and, consequently, more precise modulation of disease progression.

2.3 Signaling pathways as engineering-relevant control nodes in immunometabolic reprogramming

Within the molecular networks that govern immunometabolic reprogramming, several signaling pathways act as critical control nodes that integrate metabolic stress, hypoxic adaptation, and inflammatory signaling into a coordinated regulatory framework, thereby shaping cellular functional states and sustaining inflammatory responses [25]. Among these, the NLRP3 inflammasome represents a prototypical "sensor-to-effector" axis. Metabolic stressors such as oxLDL and free fatty acids can trigger its activation, leading to caspase-1-dependent maturation and release of IL-1β and IL-18. In both animal models and human unstable plaques, NLRP3 activation is closely associated with increased inflammatory burden and plaque vulnerability [26, 27].

HIF-1α is upregulated in the hypoxic and ROS-enriched microenvironment of advanced lesions. By promoting the transcription of glycolysis-associated genes and angiogenic factors, HIF-1α remodels local metabolic programs. At the same time, its crosstalk with NF-κB reinforces the production of inflammatory cytokines, positioning HIF-1α as a cross-system node linking hypoxia, metabolism, and inflammation [28, 29]. NF-κB serves as a central hub for chronic inflammation and immune cell recruitment. It induces a broad spectrum of pro-inflammatory mediators and upregulates adhesion molecules such as intercellular adhesion molecule-1 (ICAM-1) and vascular cell adhesion molecule-1 (VCAM-1), thereby promoting leukocyte adhesion and transendothelial migration. Sustained NF-κB activation is closely correlated with increased plaque burden, and therapeutic strategies targeting upstream kinases or transcriptional activity inhibition continue to advance [30, 31]. Collectively, NLRP3, HIF-1α, and NF-κB form an interconnected regulatory network with pronounced

spatial heterogeneity in their activation patterns. Prioritizing these signaling nodes provides a robust conceptual foundation for translating omics-based mechanistic insights into engineering-driven, spatially precise therapeutic intervention strategies.

2.4 Spatial heterogeneity of the plaque microenvironment as an engineering information carrier

Beyond cellular lineages and molecular pathways, atherosclerotic plaques exhibit pronounced 3D spatial heterogeneity, which directly shapes local immunometabolic states and therapeutic responsiveness. Conventional histological sectioning provides valuable morphological information but remains insufficient for resolving coordinated interactions among cells, signaling pathways, and metabolic programs within spatially confined microdomains [32]. In contrast, spatial transcriptomics (ST) and multimodal imaging technologies now enable high-resolution mapping of immune cell distribution, metabolic activity, and pathway activation across distinct plaque regions, such as the fibrous cap, necrotic core, and shoulder areas [10].

Spatially resolved studies increasingly demonstrate that plaque shoulder regions are enriched in activated T cells and pro-inflammatory macrophages, whereas the necrotic core is dominated by foam cells characterized by high lipid burden, reduced metabolic activity, and features of iron accumulation. These regional differences define an operational target map for region-oriented intervention strategies [9, 33]. For example, regions with high HIF-1α expression frequently overlap with areas of low perfusion, while inflammatory shoulder regions enriched in macrophages and characterized by high VCAM-1 expression can serve as spatially defined targets for the delivery of anti-inflammatory agents or regulatory RNAs [9, 34]. Importantly, spatial heterogeneity also displays dynamic temporal characteristics. During disease progression, spatial expression patterns may shift from NF-κB-dominated inflammatory states toward HIF-1α-driven hypoxic and metabolic adaptation programs [35, 36] (Fig. 2 [37–43], Table 1 [9, 21, 26, 30, 37, 44–48]). Consequently, spatial information should no longer be viewed as a purely descriptive feature but rather as an information carrier that can be directly integrated into engineering decision-making. Such information enables precise identification of where and when specific immunometabolic programs predominate, thereby guiding the design of region-specific and temporally adaptive nanoplatforms and scaffold systems, and supporting the implementation of closed-loop intervention strategies.

3 Application of multimodal omics in mechanistic investigation

3.1 Single-cell and spatial omics as tools for cellular and regulatory decision-making

With continued technological advances, it has become evident that

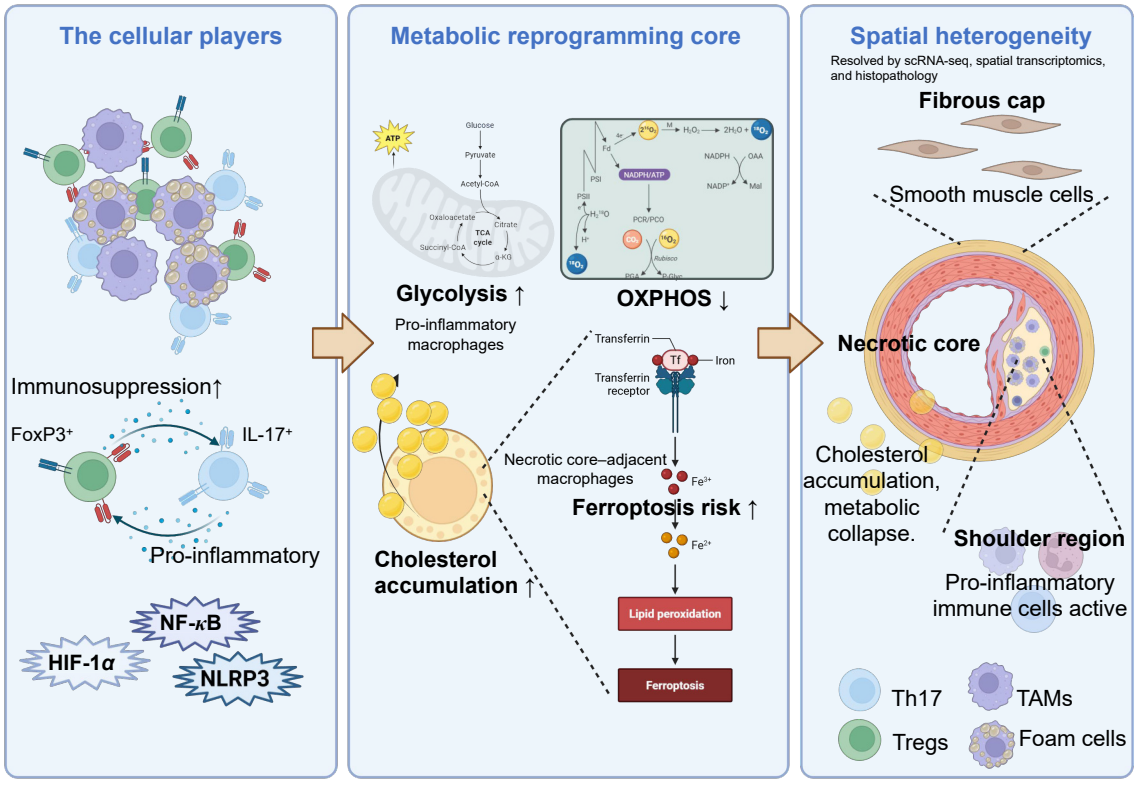

Figure 2 Integrated schematic of immunometabolic reprogramming mechanisms and signaling pathways in CA. This schematic summarizes the functional balance among immune cell subpopulations within atherosclerotic plaques, including regulatory T cells (Tregs), T helper 17 (Th17) cells, tumor-associated macrophages (TAMs), and foam cells [37, 38]. Together, this balance determines the dynamic interplay between pro-inflammatory and immunosuppressive responses within plaques [39, 40]. Core metabolic features include enhanced glycolysis, impaired mitochondrial oxidative phosphorylation (OXPHOS), cholesterol accumulation, and increased susceptibility to ferroptosis [41]. Key signaling pathways, NLRP3, HIF-1α, and NF-κB, cooperatively regulate immune activation and metabolic reprogramming [42, 43]. The right panel further highlights the spatial heterogeneity among distinct plaque microdomains, including the fibrous cap, necrotic core, and shoulder regions, illustrating their region-specific cellular compositions and metabolic states.

Table 1 Overview of key immunometabolic pathways and potential therapeutic targets in CA[a]

Module	Key components/pathways	Functional roles	Mechanistic features	Potential intervention strategies
Immune cell subsets	Foam macrophage-like subsets (e.g., TREM2$^+$/lipid-associated macrophages) [37]	Pro-inflammatory and phagocytic dual functions; drive plaque progression	Associated with high lipid load, strong phagocytic activity, and plaque instability	Modulate macrophage polarization; inhibit foam cell formation
	Tregs [44]	Anti-inflammatory; maintain immune homeostasis	Decreased density in unstable plaques	Restore Treg function via IL-2 or immunomodulators
	Th17 cells [45]	Pro-inflammatory; enhance immune responses	Increased abundance in unstable plaques; associated with heightened inflammation	Inhibit IL-17 pathway; block Th17 differentiation
Metabolic pathways	Glycolysis/OXPHOS imbalance [21]	Pro-inflammatory macrophages rely on glycolysis; anti-inflammatory subtypes prefer OXPHOS	Metabolic state determines immune cell polarization	Target metabolic regulators (e.g., HIF-1α inhibitors, AMPK activators)
	Cholesterol metabolism dysfunction (ABCA1) [46]	OxLDL and oxidized cholesterol accumulation → foam cell formation	Trigger inflammatory spread; worsen plaque instability	Enhance cholesterol efflux (via ABCA1/LXR agonists, PCSK9 inhibitors)
	Ferroptosis [47]	Iron accumulation and lipid peroxidation → cell death	Undermine fibrous cap stability; promote necrotic core formation	Use iron chelators; activate GPX4
Signaling pathways	NLRP3 Inflammasome [26]	Link metabolic stress with immune activation	Trigger IL-1β and IL-18 release upon activation	NLRP3 inhibitors (e.g., MCC950)
	HIF-1α [48]	Mediate hypoxia response; regulate glycolysis and angiogenesis	Upregulate GLUT1/HK2 and induce VEGF expression	HIF-1α inhibitors; combine with anti-angiogenic therapies
	NF-κB [30]	Central transcription factor in chronic inflammation	Activate TNF-α, IL-6, MCP-1; upregulate ICAM-1/VCAM-1	IKK inhibitors; NF-κB signaling modulators
Spatial heterogeneity	Fibrous cap region [9]	Structural stability; partial metabolic activity	High expression of Tregs and ABCA1	Targeted therapies or stents that preserve fibrous cap integrity
	Necrotic core [9]	Enriched in foam cells and iron ions	Low metabolic activity; accumulation of HIF-1α and NLRP3	Interventions targeting ferroptosis and inflammasome pathways
	Shoulder region [9]	Rich in Th17 cells and pro-inflammatory macrophages	High expression of VCAM-1/ICAM-1; strong inflammatory activity	Targeted delivery of anti-inflammatory RNAs or therapeutic antibodies

[a]AMPK: AMP-activated protein kinase; LXR: liver X receptor; PCSK9: proprotein convertase subtilisin/kexin type 9; GLUT1/HK2: glucose transporter 1/hexokinase 2; VEGF: vascular endothelial growth factor; MCP-1: monocyte chemoattractant protein-1; IKK: IκB kinase.

coronary atherosclerotic plaques exhibit substantial complexity and heterogeneity at the cellular composition level. Accordingly, single-cell and spatial omics approaches have evolved from descriptive atlases into upstream decision-making tools that enable the identification, at cellular resolution, of functionally dominant cell populations and states most relevant for precise therapeutic intervention [10, 49]. Within this framework, single-cell RNA sequencing (scRNA-seq) not only defines immune and stromal cell lineages but also reveals pronounced phenotypic plasticity of VSMCs. For example, the C5 VSMC subpopulation, characterized by transdifferentiation potential, has been linked to interactions with macrophages and extracellular matrix (ECM) remodeling. These properties indicate that such cells may represent suitable targets for functional reprogramming rather than elimination, thereby supporting intervention strategies aimed at preserving or restoring plaque structural integrity instead of inducing cell depletion [50].

ST platforms, such as GeoMX® and CosMx™, further anchor gene expression profiles within intact tissue architecture, enabling direct interrogation of cellular state dynamics and spatial distributions across plaque microdomains, including the fibrous cap, necrotic core, and shoulder regions. Through trajectory inference and annotation frameworks, these technologies allow the reconstruction of cell-state transitions across different stages of plaque development [51–53]. Integration of scRNA-seq with ST further enables the reconstruction of spatially ordered intercellular communication networks, resolving interactions among VSMC subpopulations, macrophages, and endothelial cells along spatially constrained ligand-receptor axes that cooperatively drive inflammatory amplification and tissue remodeling. Through this integration, spatially restricted interaction maps are converted into engineering-actionable information that informs the rational design of nanotechnology-based targeting strategies and scaffold-guided interventions, while providing critical upstream inputs for closed-loop precision therapeutic frameworks [54].

3.2 Epigenomic approaches as regulatory-layer inputs for precision intervention

After cellular heterogeneity has been defined, epigenomic information provides critical insight into the mechanisms underlying cell-state transitions and identifies regulatory nodes that are amenable to targeted reprogramming. In this context, the epigenomic layer serves as a key interface for translating multimodal omics data into actionable intervention strategies. Single-cell ATAC sequencing (scATAC-seq) and CUT&Tag profiling enable high-resolution characterization of state-specific

chromatin accessibility landscapes and transcription factor binding patterns, thereby offering regulatory explanations for cell-state transitions observed in cardiovascular disease [55]. Integrated analysis of scRNA-seq and scATAC-seq captures phenotypic transitions among immune cells and smooth muscle cell (SMC) subpopulations while simultaneously identifying the dynamic regulatory programs that drive these transitions. For example, stress-associated regulatory circuits centered on activating transcription factor 3 (ATF3) have been shown to govern SMC phenotypic switching and adaptive responses, providing mechanistic insight into lineage plasticity within atherosclerotic lesions [56–58]. Further reconstruction of gene regulatory networks (GRNs) integrates transcriptomic and epigenomic signals into testable regulatory models, enabling system-level dissection of how regulatory elements cooperatively shape cellular behavior. These approaches facilitate the identification of targetable transcription factors, enhancer regions, and regulatory motifs, thereby defining "regulatory-layer anchor points" for the design of nanoplatforms and scaffold systems aimed at reprogramming specific cellular states [59, 60]. Building upon these advances, network modeling and dynamic simulation focused on the plaque microenvironment are increasingly being applied to elucidate the system-level evolution of immunometabolic reprogramming and to support predictive, controllable intervention strategies [61, 62].

3.3 Modeling microenvironmental interactions as network-layer inputs for precision intervention

After cellular lineages and regulatory mechanisms have been defined, intercellular communication networks emerge as a critical "network-layer input" for translating omics discoveries into actionable intervention strategies. Computational frameworks such as CellChat and NicheNet infer ligand–receptor mediated signaling interactions from multimodal omics data, enabling systematic reconstruction of the strength and directionality of communication among immune cells, stromal cells, and endothelial cells within atherosclerotic plaques [63, 64]. CellChat-based analyses of atherosclerosis datasets have identified key communication nodes between macrophages and endothelial cells, as well as between macrophages and VSMCs, highlighting pathway modules that exert disproportionate influence on inflammatory amplification and structural remodeling [10, 65]. NicheNet further links "ligand–receptor events" to downstream "target gene transcriptional responses". For example, transforming growth factor beta 1 (TGFB1)-centered signaling networks have been shown to concurrently regulate ECM remodeling, phenotypic switching, and inflammatory state transitions, thereby providing a principled basis for prioritizing targets at the network level [56, 57]. Accordingly, layered interaction maps generated through multi-tool integration can be viewed as engineering-relevant blueprints that indicate where and how regulatory perturbations are most likely to produce maximal system-level effects. These maps provide essential guidance for the early-stage design of nanodelivery systems, 3D printing strategies, and region-specific intervention platforms (Fig. 3, and Table 2 [8, 60, 65–68]). As spatially resolved and multimodal datasets continue to mature, an increasing number of high-risk pathways are being shown to exhibit both spatial restriction and subtype specificity. Prioritizing pathway modules defined by the combined dimensions of spatial localization, cell-type specificity, and network topology will be a key step in translating multi-omics discoveries into closed-loop, engineering-driven precision intervention strategies.

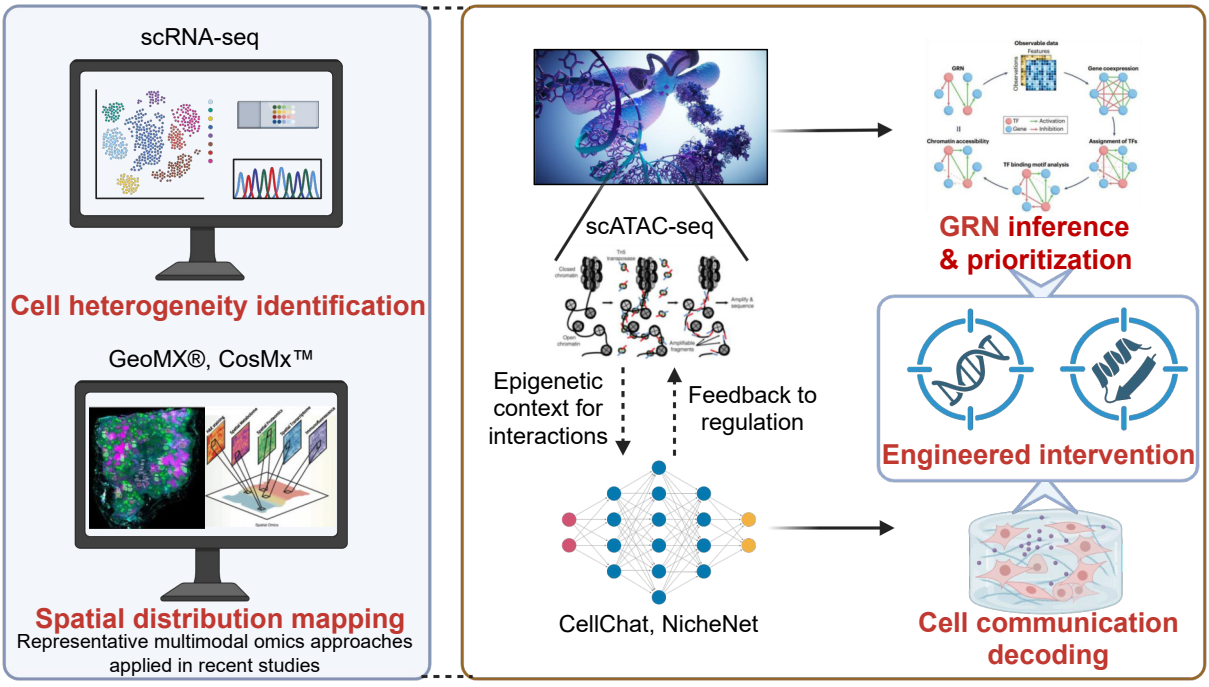

Figure 3 Integrated analytical workflow of single-cell, spatial omics, and epigenomics in coronary atherosclerosis. This workflow illustrates how single-cell RNA sequencing (scRNA-seq) and spatial transcriptomics platforms (such as GeoMX® and CosMx™) are used to identify cellular heterogeneity and spatial organization within coronary atherosclerotic lesions. Epigenomic analyses, including scATAC-seq and CUT&Tag, are subsequently applied to characterize chromatin accessibility landscapes and transcription factor binding patterns. These data are further integrated with computational modeling tools, such as CellChat and NicheNet, to infer intercellular communication networks and reconstruct GRNs. Collectively, this integrative framework supports the identification of spatially and functionally relevant therapeutic targets and provides a rational foundation for the design of engineering-driven intervention strategies. CUT&Tag: Cleavage Under Targets and Tagmentation.

Table 2 Summary of commonly used multimodal omics tools and databases in CA research

Technology category	Tools/databases	Analytical dimension	Typical applications	Advantages	Limitations
Single-cell transcriptomics (scRNA-seq) [66]	10× Genomics, smart-seq2	Cell lineage tracing, transcriptional states	Identification of novel VSMC subpopulations (e.g., C5) and TAM heterogeneity	High resolution; enables detection of rare cell types	High cost; lacks spatial context
Spatial transcriptomics [8]	10× Visium, NanoString GeoMX®, CosMx™	Spatial gene expression and microenvironment structure	Reveals spatial heterogeneity of fibrous cap, necrotic core, and shoulder regions	Accurate spatial dimension; integrates structure and function	Limited resolution; single-cell spatial resolution is still developing
Epigenomics (scATAC-seq, CUT&Tag) [67]	10× ATAC, CUT&Tag	Chromatin accessibility, regulatory elements	Identifies key enhancers and transcription factors involved in SMC transdifferentiation	Reveals transcription factor activity and chromatin dynamics	Limited application in CA-specific studies
Multi-omics integration and gene regulatory networks (GRNs) [60]	Seurat v5, SCENIC, Monocle3	Cross-omics correlation, trajectory inference, network modeling	Constructs intracellular GRNs; infers lineage trajectory and regulatory axes	Integrates scRNA-seq with ATAC-seq to elucidate regulatory circuits	High algorithmic complexity; computationally intensive
Cell-cell communication modeling [65]	CellChat, NicheNet	Ligand-receptor pathway prediction, intercellular signaling	Maps immune-VSMC communication networks; predicts inflammatory signaling axes	Visualizes interaction networks; facilitates target discovery	Relies on known databases; predictions require experimental validation
Multicenter omics databases [68]	Human Cell Atlas, Single Cell Portal, CardioAtlas	Integrated multi-cohort, multi-platform omics datasets	Constructs CA-specific cellular atlas; supports external validation	Standardized public datasets; supports large-scale analysis	Data heterogeneity; limited clinical stratification of patients

3.4 Key challenges and translational bottlenecks in multimodal omics integration

Despite the unprecedented resolution and information density provided by multimodal omics, substantial structural barriers remain when these datasets are used as "upstream decision inputs" for precision intervention. Addressing these challenges is essential for achieving meaningful translational impact. One major limitation arises from data heterogeneity, which stems from differences in disease stage, sampling location, surgical procedures, tissue processing and dissociation protocols, cell recovery bias, and inter-individual variability. Together, these factors can substantially alter cell-type proportions and state distributions, thereby reducing comparability across cohorts. A second challenge relates to cross-platform noise and measurement bias. For example, scRNA-seq and ST differ systematically in resolution, capture efficiency, and background signal. In addition, distinct ST platforms employ different probe designs and signal deconvolution strategies, which can lead to inconsistent representations of the same biological state. Such discrepancies undermine the robustness of cell-type mapping, state-transition inference, and intercellular communication network reconstruction. Third, limitations in standardization and reproducibility further constrain translational utility. These issues are reflected in inconsistent cell annotation frameworks, wide variation in quality control thresholds and batch-correction strategies, the absence of unified criteria for defining spatial regions, and discordant outputs across cell-cell communication analysis tools. As a result, instability can arise in target prioritization, which poses a particular challenge when engineering decisions depend on reliable and reproducible ranking of actionable nodes. Finally, limited sample size represents a pronounced constraint in coronary artery research. High-quality human coronary plaque specimens are difficult to obtain, often resulting in small cohorts, insufficient stratification, and a lack of longitudinal sampling. These factors reduce statistical power for detecting rare cell states, spatially restricted microdomain signals, and causal trajectories, and they limit the generalizability of derived models. In light of these challenges, more translatable multimodal omics strategies should emphasize multicenter study designs, paired sampling (i.e., multimodal data matched within the same patient), standardized experimental and analytical workflows, and the development of shared reference atlases. Importantly, orthogonal validation approaches, including immunohistochemistry, multiplex imaging, and functional assays, are essential for converging computational inferences into testable mechanisms. Together, these measures are critical for ensuring that omics-derived outputs can reliably inform the parameterized design, and closed-loop optimization of nanodelivery and scaffold-based intervention systems.

4 Multi-omics-guided discovery of therapeutic targets

Building upon the mechanistic framework established in Section 2 and the omics-based analytical strategies outlined in Section 3, this section focuses on how multimodal omics technologies enable the spatially resolved discovery, prioritization, and validation of therapeutic targets in CA. Specifically, the integrated application of single-cell transcriptomics, ST, and epigenomic profiling allows for the systematic identification of molecular targets that exhibit functional dominance, spatial heterogeneity, and practical accessibility for intervention. Through this integrative approach, multi-omics analyses establish a direct conceptual link between mechanistic insight and the engineering-driven design of precision therapeutic strategies.

4.1 Multi-omics-guided identification of spatially actionable targets: NLRP3, HIF-1α, triggering receptor expressed on myeloid cells 2 (TREM2), ATP-binding cassette transporter A1 (ABCA1), and related molecules

In recent years, the widespread application of single-cell and spatial omics technologies has enabled high-resolution dissection of the pronounced heterogeneity within the microenvironment of coronary atherosclerotic plaques [69]. Unlike conventional target screening approaches based solely on differential expression, multi-omics strategies allow candidate targets to be prioritized according to cell-type specificity, spatial localization patterns, and regulatory centrality. This integrative framework provides a robust theoretical

and experimental basis for the development of precision intervention strategies [22, 70].

With the deep integration of multi-omics into mechanistic studies, their value in target discovery and spatial validation has become increasingly evident. Previous studies have demonstrated that activation of the NLRP3 inflammasome markedly enhances the release of pro-inflammatory cytokines such as IL-1β, promotes macrophage polarization toward inflammatory phenotypes, and accelerates plaque progression [71]. ST analyses comparing stable and progressive plaques have further revealed elevated NLRP3 expression within immune-enriched microdomains, particularly in regions densely populated by macrophages and monocytes [72, 73]. If future high-resolution ST datasets further confirm these differential localization patterns, NLRP3 may serve not only as a biomarker of high-risk plaques but also as a spatially addressable therapeutic target.

Similarly, HIF-1α, a transcription factor central to hypoxic responses, has attracted considerable attention in plaque biology. Local hypoxia and metabolic stress stabilize HIF-1α protein within plaques, inducing the expression of glycolytic enzymes and pro-angiogenic factors such as VEGF, thereby promoting neovascularization and metabolic adaptation [8]. When combined with spatial omics or high-resolution tissue localization techniques, HIF-1α expression can be precisely mapped to high-risk regions such as the necrotic core and plaque shoulder, strengthening its suitability as a spatially defined intervention target. These effects facilitate immune cell recruitment and exacerbate local metabolic imbalance [74, 75]. Moreover, omics analyses indicate that HIF-1α-high cell populations are often enriched at the margins of the fibrous cap, with spatial distributions closely overlapping regions prone to restenosis [76]. This pattern suggests that HIF-1α modulation may be more appropriate for region-specific delivery strategies rather than systemic inhibition.

Beyond inflammation- and hypoxia-related pathways, TREM2 has emerged as a key regulator of macrophage phenotypic stability. TREM2-positive macrophage subsets display enhanced cholesterol uptake, lipid handling capacity, and self-renewal potential, thereby contributing to the maintenance of foam cell-like states within plaques [37, 77–79]. These cells are thought to exert a stabilizing influence on the microenvironment surrounding the necrotic core [80], and their characteristic spatial localization provides clearly defined target zones for precision intervention.

Finally, ABCA1, a central regulator of cholesterol efflux and high-density lipoprotein biogenesis, represents an additional metabolically actionable target [46, 81]. Downregulation of ABCA1 expression has been associated with increased foam cell accumulation and aggravated lipid deposition across multiple experimental models [82, 83]. Accordingly, when spatial omics data are integrated with functional validation, ABCA1 represents a highly promising spatial intervention target at the metabolic level (Fig. 4) [84].

Taken together, the identification of targets such as NLRP3, HIF-1α, TREM2, and ABCA1 illustrates how multi-omics approaches can transform highly heterogeneous molecular signals into spatially resolved "target maps". By anchoring target discovery to cell-type specificity, spatial localization, and regulatory dominance, multi-

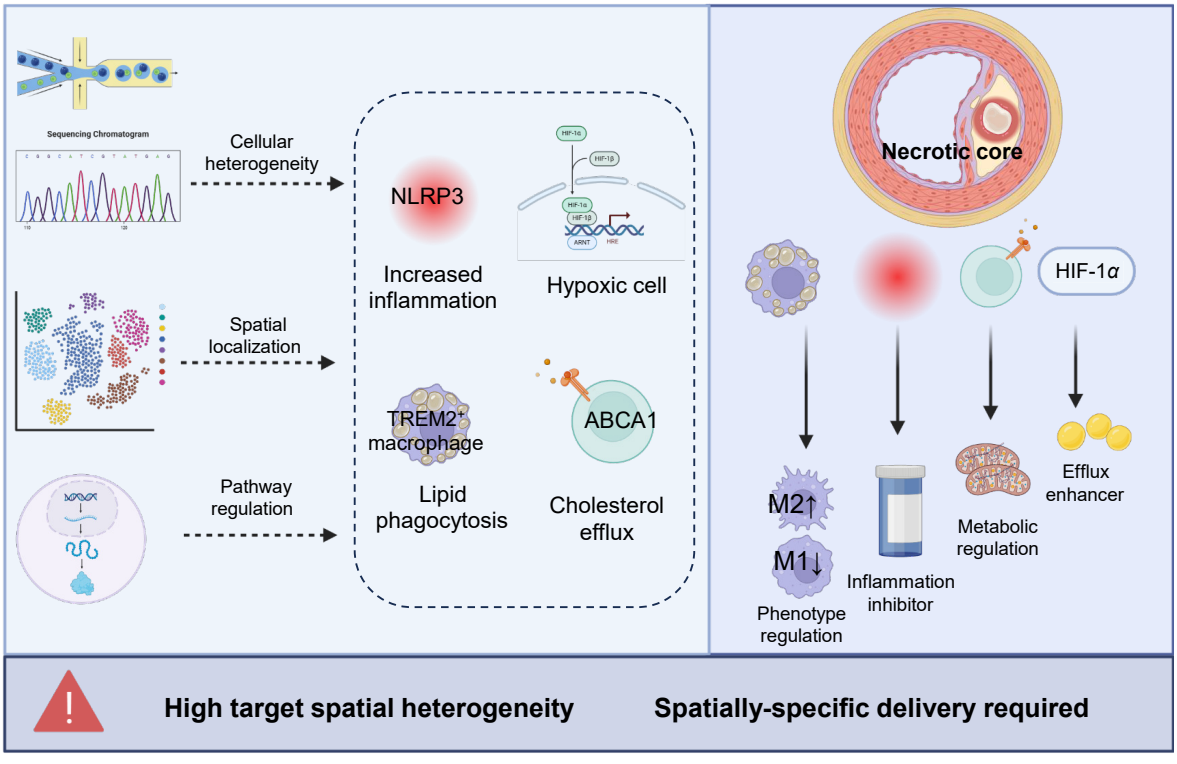

Figure 4 Schematic of target identification and intervention strategies supported by multimodal omics. Multimodal omics approaches—including scRNA-seq, ST, and epigenomic analyses—are employed to decipher cellular heterogeneity, spatial localization, and regulatory pathways, leading to the identification of four key targets: NLRP3, HIF-1α, TREM2, and ABCA1 [8, 46, 71, 77, 81]. These targets exhibit region-specific distributions within atherosclerotic plaques: NLRP3 is associated with heightened inflammatory responses; HIF-1α mediates hypoxic adaptation; TREM2 regulates macrophage lipid uptake; and ABCA1 facilitates cholesterol efflux [8]. Based on their spatial profiles, various intervention strategies can be devised, including macrophage phenotype modulation (M1/M2), anti-inflammatory agents, metabolic regulators, and cholesterol efflux enhancers. The lower section underscores the necessity of addressing both the spatial heterogeneity of targets and region-specific delivery in CA interventions. M1: classically activated macrophage; M2: alternatively activated macrophage.

omics-guided strategies provide a rational foundation for the downstream design of nanodelivery systems and 3D printed scaffolds, thereby accelerating the translation of mechanistic insights into precise, engineering-driven therapeutic interventions.

4.2 Spatial specificity and precise cell-lesion matching for targeted intervention

Following the identification of therapeutic targets, a major translational bottleneck lies in achieving precise spatial alignment among molecular targets, dominant cellular subpopulations, and high-risk lesion microdomains. This alignment represents a prerequisite for clinically actionable precision therapy [85]. ST and spatially resolved molecular profiling technologies enable the delineation of target distribution at tissue- and subregion-level resolution, thereby providing quantifiable design principles for "region-oriented delivery" strategies [85, 86]. Accumulating evidence indicates that many immunometabolic targets exhibit pronounced spatial heterogeneity. HIF-1α is typically localized to hypoperfused and hypoxic regions, NLRP3 preferentially accumulates within immune cell-dense inflammatory niches, and TREM2 shows strong spatial association with macrophage-enriched boundary zones surrounding the necrotic core [87–89]. These spatial patterns provide a direct rationale for integrating molecular targeting with region-specific delivery strategies.

Although a fully closed-loop experimental pipeline spanning spatial localization, target identification, targeted nanocarrier design, and region-restricted delivery have not yet been comprehensively implemented in CA, an expanding body of evidence supports the feasibility of this approach. For example, TREM2-positive foam cell-like macrophages exhibit sustained high expression within plaques and show close associations with necrotic core expansion and plaque instability, highlighting their potential as region-specific intervention targets [37, 90]. Similarly, HIF-1α represents a spatially constrained target whose activity is largely restricted to hypoxic microdomains. Selective delivery of HIF-1α inhibitors or pathway modulators to these regions may enable coordinated regulation of metabolic stress and pathological angiogenesis while minimizing systemic side effects [91–93].

More broadly, the principle of spatial specificity can be elevated to a "cell-lesion coupling" design paradigm, in which cellular identity, anatomical location, and functional output are jointly incorporated into therapeutic decision-making [94]. Recent 3D "cell-location-function" interaction maps have shown that ABCA1 activity is more closely associated with endothelial cells within the fibrous cap, whereas NLRP3 expression is concentrated in stromal immune cell clusters in plaque shoulder regions. These findings provide a methodological framework for matching "cell type-region-strategy" in targeted intervention design [95]. Overall, spatial specificity and precise cell-lesion matching transform multimodal omics data from descriptive atlases into engineering constraints. By explicitly addressing where pathogenic programs arise and which cell populations dominate high-risk regions, this approach lays the foundation for individualized, region-specific targeted interventions and advances the translational application of precision, engineering-driven therapeutic platforms in CA (Table 3 [72, 96–101]).

4.3 Translational pathway from target discovery to engineering-based intervention

With the deepening application of multimodal omics in CA research, target identification has evolved from traditional differential expression-based screening into an integrative selection framework that jointly evaluates cell-type specificity, spatial localization, and functional relevance [9, 53]. Leveraging scRNA-seq and ST, researchers have not only delineated the expression profiles of key regulatory molecules, such as NLRP3, HIF-1α, TREM2, and ABCA1, but have also elucidated their spatial distribution across specific cellular subpopulations and lesion microdomains [69, 77]. For instance, TREM2-positive macrophages preferentially localize to the margins of the necrotic core, whereas HIF-1α expression is markedly enriched in hypoxic, low-perfusion microregions within plaques. These spatial patterns establish a clear framework for precision therapeutic design [9, 77, 102].

The incorporation of epigenomic analyses and intercellular communication modeling tools, including scATAC-seq, CellChat, and NicheNet, has further shifted translational research from isolated target identification toward network-level interrogation of regulatory programs, ligand–receptor signaling, and cross-cellular interactions [63]. This perspective reframes therapeutic targets as integral components of spatially organized, multicellular regulatory networks rather than as isolated intracellular effectors. For instance, ABCA1 not only mediates cholesterol efflux but also contributes to

Table 3 Spatial characteristics and therapeutic strategies of omics-identified targets in coronary atherosclerosis[a]

Target	Functional mechanism	Associated cell types	Therapeutic strategy	Validation stage
NLRP3 [72]	Activates inflammasome, promotes IL-1β release, enhances local inflammation	Pro-inflammatory macrophages (M1)	Small-molecule inhibitors targeting NLRP3 activation	Preclinical animal studies
HIF-1α [96]	Upregulates glycolytic enzymes, induces angiogenesis, regulates metabolic imbalance	Macrophages, endothelial cells	Local delivery of HIF-1α inhibitors (e.g., Echinomycin)	Preclinical animal studies
TREM2 [97]	Stabilizes foam macrophages, enhances cholesterol clearance and phagocytosis	Foam cell-like macrophages	Nanoparticle-based delivery targeting TREM2	Preclinical evidence available
ABCA1 [98]	Mediates cholesterol efflux, HDL synthesis, and foam cell reversal	SMCs, macrophages, endothelial cells	Agonists (e.g., LXR activators) to enhance ABCA1 expression	Animal models and exploratory clinical observations
VCAM-1 [99]	Promotes monocyte adhesion and migration, aggravates inflammation	Endothelial cells	Antibody blockade or targeted RNA therapies	Preclinical research
CD36 [100]	Mediates lipid uptake, facilitates foam cell formation	Macrophages	CD36 antagonists to limit lipid accumulation	Preclinical phase
IL-6R [101]	Amplifies chronic inflammatory signaling, linked to plaque instability	T cells, macrophages	Tocilizumab (IL-6R inhibitor)	Clinical trial stage

[a]HDL: high-density lipoprotein.

plaque stabilization through coordinated signaling axes linking endothelial cells, macrophages, and vascular SMCs. In contrast, NLRP3-driven inflammatory activation exhibits spatially amplified effects within immune cell-enriched plaque regions [103]. Such network- and space-aware perspectives provide a systems-level rationale for engineering-oriented therapeutic design, wherein target suitability must be evaluated simultaneously across molecular function, cellular context, and lesion geography. The spatial expression characteristics of targets and their compatibility with the surrounding microenvironment have emerged as core constraints in delivery platform design. For example, TREM2 can serve as a molecular anchor for directing therapeutic carriers toward regions adjacent to the necrotic core. The enrichment of HIF-1α in hypoxic microdomains supports the use of ROS- or pH-responsive release modules, whereas the preferential expression of ABCA1 in fibrous cap-associated regions highlights the potential value of integrating molecular modulation with biomechanical reinforcement strategies [77, 102].

Accordingly, translational intervention design must integrate multiple engineering dimensions, including molecular recognition, spatial matching, stimulus-responsive activation, and structural support, rather than optimizing individual components in isolation. This integrative logic establishes a closed-loop translational pathway encompassing identification, matching, response, and functional conversion, thereby enabling effective coupling between omics-driven target discovery and deployable engineered systems [87, 102, 104].

In summary, this integrative logic establishes a closed-loop translational pathway encompassing identification, matching, response, and functional conversion, thereby enabling effective coupling between omics-driven target discovery and deployable engineered systems. By embedding molecular targets within their corresponding cellular networks and lesion microenvironments, this strategy provides a testable and translatable conceptual foundation for next-generation engineered intervention platforms, including nanomaterial-based delivery systems and 3D printed biomimetic scaffolds. On this basis, the subsequent sections will systematically explore how intelligent intervention systems integrate molecular recognition, stimulus-responsive release, and biomechanical functionality to bridge mechanistic understanding with clinical application.

5 Engineering-based intervention strategies: integration of nanocarrier delivery and 3D scaffold applications

Building upon the identified immunometabolic targets and spatially heterogeneous microdomains, the construction of engineering-based intervention platforms urgently requires the coordinated integration of structural design, drug delivery, and biomechanical support. This section focuses on the engineering characteristics of nanomaterial-based systems and 3D-printed biomimetic scaffolds, with systematic analysis of their key design parameters, including molecular recognition, material responsiveness, controlled release behavior, mechanical properties, and biodegradability. Emphasis is placed on the physical translation pathway "from target identification to structural implementation". Intelligent system strategies, including AI-assisted design and intervention simulation, will be discussed in details in Section 6.

5.1 Nanoplatform design and targeted modification (e.g., ICAM-1, VCAM-1)

Atherosclerotic lesions exhibit pronounced spatial heterogeneity and cell-specific marker expression, providing a theoretical basis for targeted drug delivery strategies. To achieve precise delivery to specific cellular subpopulations, recent studies have focused on endothelial adhesion molecules, particularly ICAM-1 and VCAM-1, as primary targeting ligands [105, 106]. In one animal model study, surface modification of nanoparticles with the LFA-1 I-Domain significantly enhanced adhesion to ICAM-1-enriched endothelium and increased local drug accumulation [107]. The high affinity between these adhesion molecules and their ligands offers a robust basis for targeted intervention within inflammatory microenvironments.

Beyond ICAM-1, VCAM-1 represents another promising target due to its widespread upregulation during endothelial activation in atherosclerotic arteries [108]. Lipid-based nanocarriers functionalized with the VHPK peptide have been shown to selectively recognize VCAM-1-positive regions, enabling targeted delivery of anti-inflammatory RNA-based therapeutics [109, 110]. Furthermore, biomimetic strategies have been employed to enhance targeting efficacy. For instance, macrophage membrane-coated nanocarriers leverage native adhesion pathways to achieve "self-recognition" and preferential localization to inflamed vascular walls [111].

From a materials engineering perspective, nanoplatforms applied to CA primarily include lipid-based nanoparticles (LNPs), polymeric nanoparticles (such as poly(lactic-co-glycolic acid) (PLGA)- or PEGylated systems), and biomimetic membrane-coated nanoparticles. LNPs are characterized by high encapsulation efficiency and favorable endosomal escape capability, making them particularly suitable for the delivery of nucleic acid therapeutics, including siRNA and mRNA. In contrast, polymeric nanoparticles offer tunable degradation kinetics and mechanical stability, enabling sustained and controllable release of small-molecule anti-inflammatory or lipid-modulating agents [112, 113]. Biomimetic nanocarriers, including macrophage membrane- or platelet membrane-coated nanoparticles, further exploit endogenous adhesion mechanisms and immune evasion properties, thereby enhancing plaque accumulation and prolonging circulation time under inflammatory and high-shear vascular conditions [114].

Notably, some platforms integrate both ICAM-1 and VCAM-1 targeting strategies to generate dual-modified nanosystems [115]. Such dual-targeting nanoplatforms establish a modular and programmable engineering framework in which molecular recognition units can be rationally coupled with therapeutic payloads. This design paradigm builds a critical translational bridge between plaque-specific target recognition and precision nanomedicine applications in CA [116, 117]. This "dual-ligand" design enhances target selectivity in complex marker-expression environments and reduces off-target effects. From a fully integrated perspective encompassing target selection, carrier design, and surface modification, nanoplatforms are rapidly advancing toward visualizability, tunability, and immunocompatibility.

5.2 Drug/nucleic acid delivery mechanisms and stimuli-responsive activation

Targeted delivery represents only the initial step of the therapeutic cascade, whereas achieving lesion-specific release remains one of

the central challenges in nanoplatform-enabled precision treatment. In recent years, research has shifted from single-target surface modification toward "pathology-responsive activation", in which characteristic features of inflammatory lesions, including acidic pH, ROS accumulation, and elevated inflammatory enzyme activity, are exploited to trigger structural transitions of delivery vehicles or initiate payload release. This approach reduces systemic toxicity and improves therapeutic efficacy. From an engineering perspective, pathology-responsive nanoplatforms establish a direct coupling between plaque-specific biochemical abnormalities and material-level structural transitions, thereby forming a controllable release logic of "microenvironment sensing-carrier activation-payload release". In an ApoE$^{-/-}$ mouse model, ROS-responsive nanoparticles constructed using poly(thioether) selectively released anti-inflammatory agents within atherosclerotic plaques, significantly attenuating local inflammation and foam cell formation [118, 119].

Concurrently, nucleic acid delivery platforms have emerged as a promising strategy for modulating endogenous gene networks. Existing studies indicate that siRNA- and miRNA-based silencing or activation of key regulatory genes in CA, including ABCA1, sterol regulatory element-binding protein 1 (SREBP1), and hepatocyte nuclear factor 4 alpha (HNF4α), holds multifaceted potential for controlling cholesterol metabolism, inflammatory signaling, and macrophage polarization [82]. For instance, Zhou et al. developed a cationic liposome-based mRNA delivery platform that enables targeted expression of an LXR agonist. This platform effectively induces ABCA1 expression in macrophages, promotes cholesterol efflux, and markedly enhances plaque stability in animal models [120]. Another study employed peptide-modified LNPs to deliver miR-33 inhibitors, achieving favorable tissue specificity and transcriptional regulation across multiple plaque models [120]. In addition, Kwon et al. developed a biomimetic membrane-coated siRNA delivery platform that successfully downregulated the NF-κB pathway, thereby providing a foundational tool for reshaping the immune microenvironment [121, 122].

Beyond endogenous stimuli-responsive mechanisms, exogenous activation platforms have also demonstrated potential in specific clinical contexts [123–125]. Several studies have designed thermosensitive nanoplatforms responsive to near-infrared (NIR) light, enabling site-specific drug release upon NIR irradiation. Such systems are particularly suitable for superficial arteries or regions accessible via interventional devices [126]. Magnetic-responsive systems have also been developed, allowing drug-loaded particles to be guided and concentrated under an external magnetic field, thereby enhancing targeted delivery to branched vessels or deep-seated lesions [127].

In summary, responsive delivery strategies are evolving from static "targeting" paradigms toward integrated systems that combine controlled release with dynamic feedback regulation. When coupled with target maps derived from ST and with individualized characterization of lesion features, these platforms offer a feasible engineering pathway for constructing closed-loop drug delivery systems encompassing recognition, activation, modulation, and feedback. These systems hold promise as a critical translational bridge linking multi-omics information with precision nanotherapeutic interventions for CA (Fig. 5).

5.3 3D printing materials, biomechanics, biodegradability, and biomimetic modeling

In the realm of mechanical support and structural repair, recent studies have increasingly highlighted the potential of 3D printing technology to enable highly customizable stent designs for vascular interventions. For instance, M. Shahverdi et al. employed melt electrowriting (MEW) in combination with polycaprolactone (PCL)/polyurethane (PU)/gelatin composites to fabricate small-diameter, dual-layer vascular scaffolds exhibiting low bending radii and excellent antithrombotic performance, while maintaining favorable cell adhesion and proliferation properties [128]. These scaffolds provided a foundation for structural repair by simultaneously optimizing mechanical integrity and cellular compatibility.

Concurrently, biodegradable biomaterials, such as alginate/gelatin (Alg/Gel) blends combined with ApoA-I-modified nanoparticles, have been explored for constructing scaffold platforms with inherent drug delivery potential [129]. Model-based and experimental studies have demonstrated that Alg/Gel + ApoA-I scaffolds exhibit superior biocompatibility and sustained release profiles, supporting their potential as smart scaffold systems for vascular applications [130, 131].

From an engineering perspective, biomimetic vascular scaffolds are designed to recapitulate key features of native blood vessels across three interrelated dimensions. Material-level biomimicry aims to emulate the composition and bioactivity of the ECM, thereby providing appropriate biochemical cues for cellular interaction. Structural biomimicry focuses on reproducing fiber orientation, pore architecture, and mechanical compliance to mirror the hierarchical organization and anisotropic mechanics of native vessels. Functional biomimicry enables controlled bioactive release and adaptive mechanical responses under physiological loading conditions. Collectively, these design dimensions allow biomimetic scaffolds to more faithfully reproduce the dynamic structure-function relationships of natural blood vessels [129, 132].

Regarding material selection, extensive research has assessed polycaprolactone (PCL), polylactic acid (PLA), and gelatin methacryloyl (GelMA) for their biocompatibility and degradability, ensuring that printed scaffolds can maintain mechanical support within vascular environments while undergoing controlled biodegradation [133–135]. Functionally, advanced printing strategies, including multi-nozzle coordination and co-printing of heterogeneous materials, have enabled the integration of drug loading, stress-guided microarchitecture, and localized bioactive molecule delivery, thereby improving the precision and efficacy of scaffold-based interventions [129, 136].

Notably, several 3D-printed or electrospun composite vascular grafts have demonstrated significant advantages in animal models, including enhanced endothelialization, improved antithrombotic properties, and superior mechanical compliance. For instance, Xiao et al. developed a porous 3D-printed vascular graft that exhibited robust antithrombotic capacity and efficient endothelial coverage in a murine model [132]. In another study, a gradient-structured 3D-printed graft implanted into the abdominal aorta showed faster endothelialization, improved smooth muscle layer reconstruction, and vascular compliance more closely resembling native arteries compared with electrospun scaffolds after one month [137]. Moreover, the programmable microarchitecture of these scaffolds enables integration with stimuli-responsive materials, including thermosensitive and enzyme-responsive hydrogels, thereby supporting future development of recognition–response–release therapeutic systems [138–140].

Despite these advances, several engineering challenges remain to

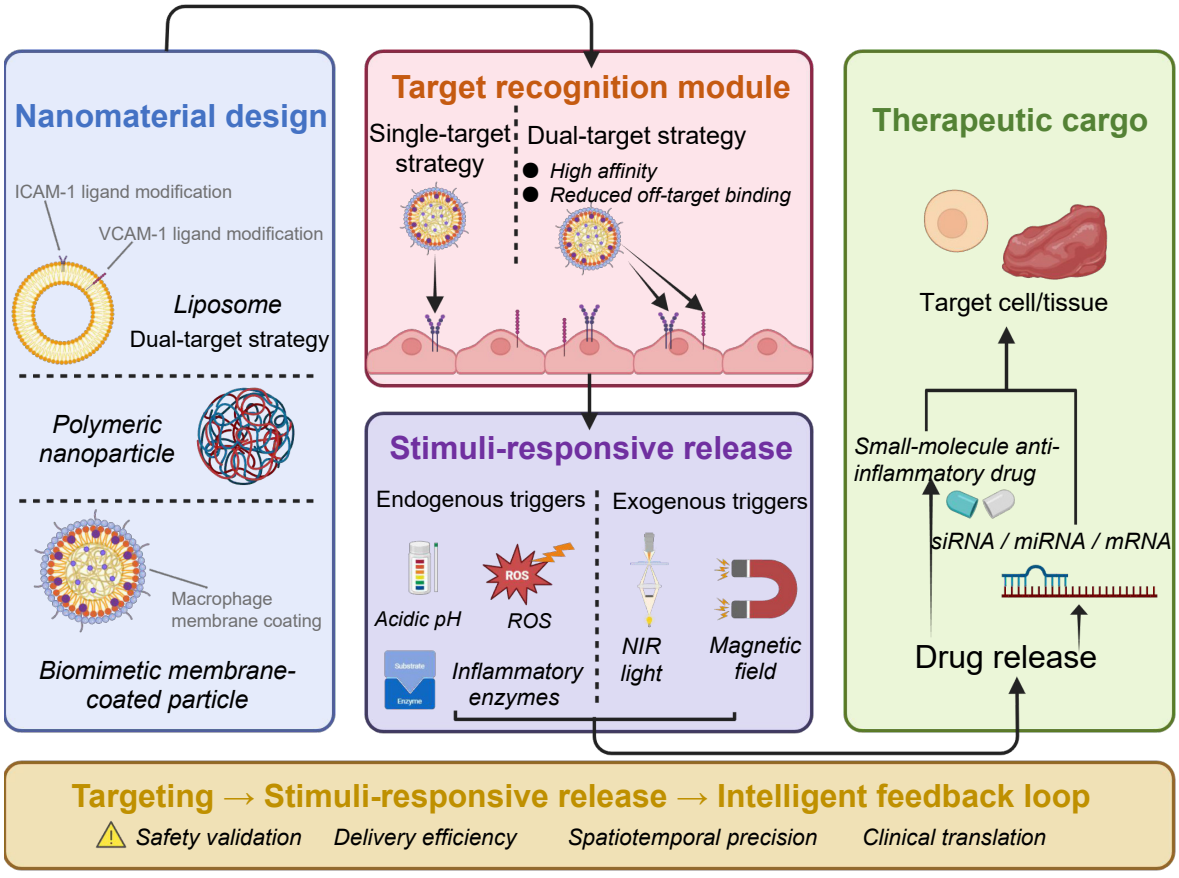

Figure 5 Schematic of nanocarrier structure and targeting mechanisms for drug delivery systems. This diagram illustrates the design and modification strategies of various nanoplatforms, including liposomes, polymeric nanoparticles, and biomimetic membrane-coated particles, featuring ligand modifications such as ICAM-1 and VCAM-1, or macrophage membrane encapsulation. The targeting module compares single-ligand and dual-ligand strategies, with the latter offering enhanced affinity and reduced off-target binding. Stimuli-responsive mechanisms are employed in the delivery phase, enabling lesion-specific release via endogenous triggers (acidic pH, ROS, inflammatory enzymes) and exogenous stimuli (NIR light, magnetic fields). The released therapeutic cargo includes small-molecule anti-inflammatory agents and various nucleic acid drugs (siRNA, miRNA, mRNA), which act on specific target cells or tissues. The lower banner summarizes the research trajectory: "targeting → responsive release → intelligent feedback loop", while highlighting key challenges such as safety validation, delivery efficiency, spatiotemporal precision, and clinical translation.

be addressed before clinical translation can be achieved. These challenges include precise control of microscale printing resolution, long-term mechanical stability under pulsatile hemodynamic loading, and temporal synchronization between scaffold biodegradation and vascular tissue regeneration [133, 135]. Addressing these challenges is critical for advancing biomimetic scaffold design from preclinical validation toward clinically deployable vascular implants.

Particularly notable are recent advances in personalization and multifunctionality. One study reported the fabrication of an intelligent, bioresorbable vascular scaffold using a customized 3D printing system. This scaffold incorporated a polymer-based wireless pressure-sensing device, offering not only mechanical support but also real-time monitoring of dynamic vascular responses [141]. Such multifunctional scaffolds represent an important step toward the development of intelligent scaffolds with integrated sensing and feedback-regulation capabilities, aligning closely with the broader concept of closed-loop intervention systems (Table 4) [128, 129, 131, 132, 134, 136–138, 142–145].

5.4 Integration of nanotechnology and 3D printing for closed-loop intervention design

To achieve precise translation from mechanistic discovery to targeted intervention, recent efforts have focused on integrating diverse therapeutic platforms into functional closed-loop systems. Nanocarriers offer advantages in molecular targeting, intracellular delivery, and payload protection, whereas 3D-printed scaffolds provide spatial guidance and localized, sustained release, representing two highly complementary capabilities [112, 146, 147].

From a systems engineering perspective, closed-loop intervention design requires coordinated integration of four core components: target identification, stimulus-responsive activation, therapeutic modulation, and feedback regulation. Within this framework, nanocarriers primarily enable molecular-level recognition and intracellular modulation, while 3D printing platforms define spatial constraints, mechanical compatibility, and release kinetics. Together, these elements form an integrated intervention loop rather than isolated functional modules, enabling synergistic and adaptive therapeutic control.

Recognizing the complementary roles of nanocarrier delivery and structural platforms, recent studies have aimed to develop hybrid systems that combine spatial precision, functional synchrony, mechanical support, and localized drug release. Several studies have reported that composite vascular grafts or stents integrating 3D printing with nanofiber technologies can successfully incorporate antithrombotic agents or small-molecule therapeutics. In animal models, these systems have demonstrated

Table 4 Overview of materials, properties, biological functions, and translational potential of tissue-engineered vascular scaffolds

Module	Sub-dimension	Example platforms or studies
Material composition [128]	Core materials	Biocompatible, biodegradable polymers such as PCL, PU, gelatin, GelMA, PLA
Material composition [131]	Functional modifications	ApoA-I-modified nanoparticles; Alg/Gel-based drug release platforms
Printing techniques [129]	Fabrication technologies	Melt electrowriting (MEW), electrospinning-assisted printing
Printing techniques [136]	Multimaterial strategies	Multi-nozzle/multimaterial co-printing; layer-by-layer structural optimization
Mechanical properties [137]	Elasticity/compliance	3D porous designs enabling flexibility and vascular compatibility
Mechanical properties [134]	Degradation kinetics	Tailored degradation synchronized with vascular remodeling, supporting staged release
Biological function [142]	Drug delivery	Scaffold-integrated ApoA-I, siRNA, and other bioactive agents
Biological function [138]	Stimuli responsiveness	Thermo-/enzyme-sensitive hydrogels responsive to lesion-specific cues
Animal model validation [132]	Endothelialization	Mouse/rabbit vascular graft models showing favorable re-endothelialization
Animal model validation [143]	Mechanical adaptation	Hemodynamic/compliance simulations confirming structural compatibility
Translational potential [144]	Clinical cases	Published cases of 3D-printed bioresorbable stent implantation with initial safety
Translational potential [145]	Intelligent systems	Integration of wireless pressure sensors for mechanical state monitoring and feedback control

excellent mechanical compatibility, enhanced endothelialization, and reduced neointimal hyperplasia. For instance, a 3D-printed electrospun PCL-PLCL-TMP vascular graft maintained patency and reduced thrombosis in a rat abdominal aorta replacement model [148]. Similarly, a biodegradable 3D-printed scaffold coated with dipyridamole-loaded nanofibers improved re-endothelialization and suppressed medial thickening in a porcine coronary artery model [149].

Incorporating functional nanoparticles into biodegradable 3D-printed vascular grafts or scaffolds has enabled localized, controlled release of therapeutic agents or bioactive factors while preserving structural integrity and endothelial support. For example, Kabirian et al. embedded nitric oxide-releasing carbon nanotube composites into degradable small-diameter 3D-printed scaffolds, achieving sustained release, enhanced endothelial cell migration, and notable antimicrobial and antithrombotic properties [150]. These hybrid platforms modulate the local microenvironment during early post-implantation phases, and support long-term tissue regeneration and structural remodeling through the combined effects of mechanical reinforcement and controlled molecular release.

Several integrated nanoparticle-scaffold systems have progressed to early clinical evaluation. For instance, PLGA nanoparticles loaded with Pitavastatin (NK-104-NP) completed a Phase I/IIa dose-escalation trial in patients with chronic limb-threatening ischemia. Intramuscular administration demonstrated acceptable safety and preliminary therapeutic efficacy [151]. Although this study did not directly target coronary atherosclerotic plaques, it provides clinical proof-of-concept for tissue-specific nanotherapeutic interventions in vascular disease and highlights the translational feasibility of such strategies.

The application of 3D printing in personalized biomimetic construction has progressed from preliminary animal validation to early clinical exploration. One group reported the first human implantation of a 3D-printed, bioresorbable, drug-eluting peripheral stent, which exhibited favorable biocompatibility and mechanical support in initial assessments [152]. These early clinical experiences underscore the translational potential of closed-loop engineering platforms.

Despite these encouraging advances, multiple system-level challenges remain, including scalable manufacturing, batch-to-batch reproducibility, long-term mechanical reliability, and precise control of scaffold biodegradation under physiological loading conditions. Addressing these issues will require standardized design principles and seamless integration of responsive nanotherapeutic functions to ensure robust closed-loop performance across diverse patient populations.

Overall, the development of closed-loop engineering strategies that integrate omics-guided target identification, nanocarrier-based therapeutic delivery, and 3D-printed structural support represents a core design paradigm for future precision interventions in CA (Fig. 6). At present, nanoplatforms and 3D-printed interventional systems already possess key capabilities, including target-specific recognition, stimulus-responsive release, and structural reconstruction. However, therapeutic outcomes ultimately depend not only on material performance but also on patient-specific factors, such as lesion morphology, hemodynamic conditions, and immunometabolic context. Accordingly, the next section will explore how AI and digital modeling approaches can be leveraged to simulate, predict, and dynamically optimize intervention pathways, enabling a critical transition from physical-layer design to system-level optimization.

6 Construction of a precision intervention platform empowered by intelligent systems

As nanocarriers and 3D-printed scaffolds increasingly demonstrate the capacity for targeted delivery and structural repair, a critical remaining challenge is the realization of individualized prediction and feedback-driven optimization of intervention pathways, which is essential for clinical translation. This section focuses on data-driven intelligent system strategies and systematically examines the potential applications of AI in material composition screening, target-lesion mapping, intervention outcome modeling, and feedback optimization. Particular emphasis is placed on the role of digital twin systems, which integrate multi-omics, imaging, and biomechanical simulation data to construct individualized digital representations of atherosclerotic lesions. These models enable a closed-loop optimization cycle encompassing pre-intervention prediction, intra-intervention adjustment, and post-intervention evaluation, thereby providing a rational and adaptive framework for precision intervention design.

6.1 AI analysis of high-risk plaques and ST features

To precisely delineate high-risk plaque regions, researchers have increasingly incorporated AI tools into the integrated analysis of Coronary Computed Tomography Angiography (CCTA) imaging

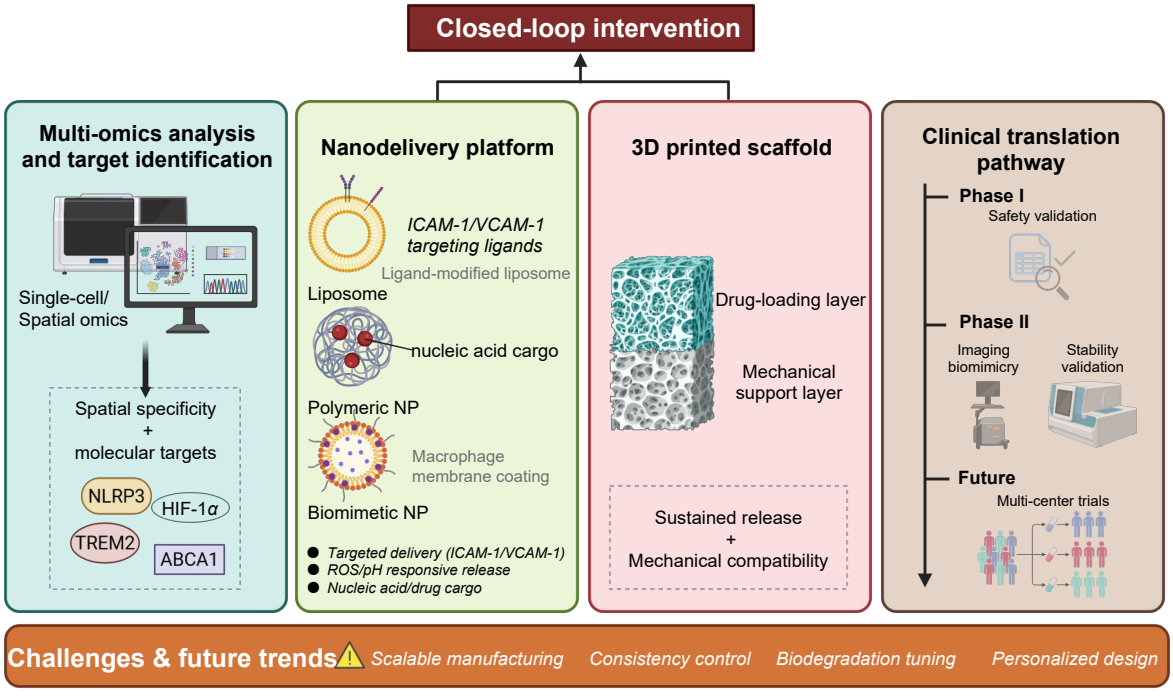

Figure 6 Schematic of the engineered closed-loop intervention system (integration of omics, targets, and platforms). Based on multi-omics analysis and target identification (NLRP3, HIF-1α, TREM2, ABCA1), this closed-loop intervention model integrates nanocarrier delivery platforms—such as liposomes, polymeric nanoparticles, and biomimetic membrane-coated particles—with ligand modifications (ICAM-1/VCAM-1) and ROS/pH-responsive release, alongside 3D-printed scaffolds composed of a drug-loading layer and a mechanical support layer. These two engineered platforms are functionally complementary: nanocarriers enable precise targeting and delivery, while 3D scaffolds offer localized, sustained release and mechanical compatibility. The right-hand section illustrates the clinical translation pathway, progressing from Phase I safety validation to Phase II imaging-guided biomimicry and stability assessment, and eventually to multicenter clinical trials. The bottom warning banner highlights future challenges and trends, including large-scale manufacturing, consistency control, biodegradability modulation, and personalized design.

and ST data. Existing studies have demonstrated that deep learning-based automated analysis of CCTA enables efficient plaque segmentation and classification, identifying vulnerable features such as lipid cores, calcification, and the napkin-ring sign. This approach significantly outperforms traditional imaging assessment methods in both automation and speed [153]. Moreover, in multicenter validations, these AI models achieved plaque scoring accuracy comparable to that of experienced angiographic specialists and showed strong predictive performance for future myocardial infarction (MI) risk [154, 155]. These advances provide a quantitative and scalable foundation for identifying high-risk microregions within atherosclerotic plaques.

Cross-disciplinary research has applied Transformer frameworks and image-molecular integration algorithms to ST feature recognition. Models such as SpatialPCA and iIMPACT have successfully inferred image-transcription features in diseases like cancer. However, in the context of atherosclerotic plaques, no published studies have yet validated AI-based predictions of TREM2-high expression regions using clinical imaging, highlighting an important direction for future research. Nevertheless, these models have demonstrated strong generalizability across multicenter datasets, suggesting that AI-based spatial analysis is approaching clinical applicability. Other studies have shown that by integrating imaging, hemodynamic, and physiological patient data, digital twin models can simulate plaque progression and treatment responses, thereby providing a dynamic platform for precision intervention modeling [156]. Additionally, cardiac digital twin models based on clinical data have been used to simulate long-term vascular changes preoperatively, offering decision support for plaque-targeted therapies [157–159]. Furthermore, ongoing studies are exploring AI applications in target selection, delivery system simulation, and response strategy optimization, establishing an intelligent link between mechanistic understanding and engineering platform design [160].

In summary, the integration of AI and digital twin technologies enables a dual-layer intelligent recognition of both high-risk plaque regions and intervention outcomes, laying the foundation for precise localization and simulation to guide subsequent intervention strategies.

6.2 Optimization pathways for smart materials and scaffold design

After identifying the target structure, the next critical step is to ensure the functional responsiveness of structural materials. Current research trends indicate growing interest in smart nanomaterials that respond to environmental stimuli such as pH, ROS, and photothermal signals, particularly for surface functionalization of cardiovascular devices [161, 162]. These materials can precisely release therapeutic agents or signaling molecules upon specific stimulation, offering the potential to combine therapeutic efficacy with structural support [163, 164].

Research teams have employed AI-driven simulation models to optimize the design of such intelligent scaffolds. Virtual simulations have been used to model mechanical behavior and drug release kinetics, enabling rapid iteration of printing parameters and systematic evaluation of scaffold stability and responsiveness under complex vascular biomechanical conditions [165]. This simulation-guided design strategy has significantly enhanced both development efficiency and structural precision.

Furthermore, integrating biodegradable biomimetic materials with stimuli-responsive delivery carriers into scaffold architectures represents a novel approach for unifying structure and function. For instance, some studies have embedded drug carriers into porous scaffolds, allowing the structure to support vascular remodeling while simultaneously delivering sustained therapeutic intervention. This dual-function design addresses the concurrent demands of tissue regeneration and targeted intervention [166].

6.3 Digital twins and personalized intervention simulation

Building upon advancements in materials and platform design, digital twin technology has emerged as a critical bridge for enabling personalized interventions [156]. Leveraging large-scale imaging datasets and recent multicenter initiatives, cardiac digital twin frameworks and virtual patient cohorts, each comprising thousands of cases, have been established to evaluate the potential outcomes of diverse intervention strategies [167]. Within this framework, researchers can prospectively assess the efficacy and associated risks of different stent designs, drug delivery systems, and combination therapies without direct patient intervention.

Notably, multimodal data integration has become pivotal to enhancing the precision of digital twin modeling. Recent studies have proposed incorporating ST, radiomics, and hemodynamic parameters into the modeling process. This integration has significantly improved predictions of plaque progression and enabled preliminary simulations of post-stent restenosis risk, offering a viable path for dynamic risk modeling [9, 168, 169]. Several clinical centers have initiated pilot programs using digital twins for preoperative planning, and early results show promising concordance between simulated outcomes and actual postoperative trajectories, supporting their potential for individualized clinical decision-making [156].

As AI and digital twin technologies become increasingly integrated, intervention paradigms are evolving toward closed-loop frameworks. Research teams have begun to explore iterative pipelines that include AI-based identification of high-risk regions, twin-driven prediction of intervention outcomes, clinical validation and feedback, and subsequent model refinement [167]. This interactive AI–Twin–Clinical paradigm provides a scalable and adaptive infrastructure for next-generation personalized precision interventions (Fig. 7).

6.4 Challenges in explainability, key bottlenecks, and regulatory pathways

Despite the considerable promise of AI and digital twin technologies in precision intervention, their "black-box" nature and the systemic uncertainties arising during integration continue to limit clinical trust and usability. The lack of interpretable model structures not only reduces clinicians' confidence in predictive outputs but may also increase the risk of misuse or inappropriate application in therapeutic decision-making [170]. Accordingly, improving model transparency and auditability has emerged as a critical prerequisite for clinical adoption. In recent years, techniques such as SHapley additive exPlanations (SHAP) value decomposition, Grad-CAM visualization heatmaps, and key-variable sensitivity analyses have been increasingly applied to cardiovascular AI models to elucidate decision logic and establish interpretable chains of evidence [171]. At the same time, closed-loop applications of AI and digital twins face several critical technical bottlenecks. First, data quality and cross-modality consistency remain persistent challenges. Variability in imaging

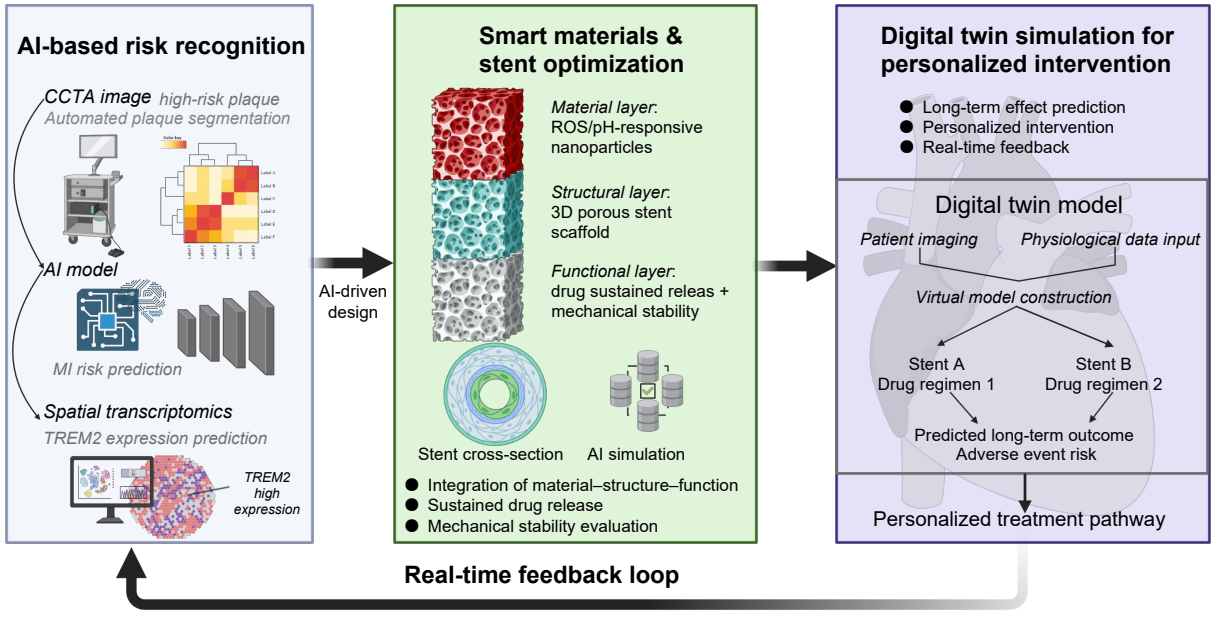

Figure 7 Schematic diagram of the AI- and omics-driven precision intervention platform. This closed-loop precision intervention pathway integrates AI with multi-omics technologies. The left panel illustrates the AI-based risk identification module, including automated plaque segmentation from CCTA, MI risk prediction via deep learning, and ST-guided detection of high TREM2 expression. The central section presents intelligent material and scaffold optimization using a three-tier design framework: a material layer (ROS/pH-responsive nanoparticles), a structural layer (3D porous scaffold), and a functional layer (sustained drug release and mechanical stability), further refined through AI-based simulation. The right panel displays the digital twin simulation, which constructs virtual patient-specific models by integrating imaging and physiological data, enabling comparison of different stent and drug regimens (e.g., Stent A/Plan 1 vs. Stent B/Plan 2), and prediction of long-term outcomes and adverse event risks. The bottom "real-time feedback loop" highlights the dynamic interplay among AI-driven identification, material optimization, and digital twin simulation, offering robust support for personalized intervention strategies.

acquisition and reconstruction protocols, segmentation standards, and omics processing pipelines can introduce distribution shifts and labeling noise, thereby complicating stable spatiotemporal alignment among omics profiles, imaging features, and hemodynamic parameters. These inconsistencies ultimately undermine model generalizability. Second, validation frameworks remain incomplete. In addition to multicenter external validation, robust mechanisms for performance drift monitoring, continuous recalibration, and adaptive updating are required. In scenarios involving combination interventions (e.g., scaffolds integrated with nanodelivery systems), a staged evidence chain is needed, encompassing algorithmic validation, parameter calibration, *in vitro* and animal benchmarking, and concordance with clinical endpoints.

From a regulatory and ethical perspective, frameworks are gradually taking shape across different regions. In the United States, the U.S. Food and Drug Administration has incorporated cardiovascular AI-assisted imaging tools into its approval pathways, emphasizing multicenter clinical validation of efficacy and safety [172]. In Europe, the European Medicines Agency places greater emphasis on data transparency and algorithm traceability while promoting harmonized validation standards across multinational cohorts [173]. In China, the National Medical Products Administration is exploring a "regulatory sandbox" model that allows early-stage validation of AI and digital twin platforms under strict ethical oversight and data security requirements [174–176]. In addition, data security and privacy protection are fundamental prerequisites for the deployment of closed-loop systems. The ability to enable cross-center data sharing while safeguarding patient privacy will largely determine whether digital twin models can be continuously iterated and optimized. Overall, the large-scale application of AI and digital twin systems will depend not only on model performance, but also on the concurrent fulfillment of requirements for explainability and uncertainty quantification, data standardization and quality control, multi-stage validation evidence chains, and regulatory compliance with ethical oversight. Achieving a sustainable balance among interpretability, safety, and clinical benefit will be essential for their successful translation into routine clinical practice.

7 Clinical translation pathways and future outlook

7.1 Challenges and successes in the clinical translation of nanomedicines (immunogenicity and industrialization)

Although nanomedicine platforms have demonstrated excellent targeting and release capabilities in laboratory settings, their clinical translation continues to face several critical challenges, particularly in the areas of immunogenicity, safety, and manufacturing consistency. In the context of CA, these limitations may result in variable therapeutic efficacy or unintended immune activation, thereby constraining broader clinical adoption [177].

Nonetheless, certain nanocarrier systems have successfully advanced into early clinical validation stages. Initial safety evaluations of targeted delivery vehicles have demonstrated their capacity to localize therapeutic agents within plaque tissues without inducing significant systemic adverse effects [178]. These findings provide an important foundation for the clinical implementation of nanotherapeutic platforms. However, large-scale clinical trials and long-term safety assessments remain essential for further validation.

In addition, the industrialization pathway represents a central determinant of translational success. Standardized manufacturing workflows, rigorous quality control systems, and regulatory compliance form the structural basis for the scalable commercialization of nanomedicine platforms [179]. Moving forward, successful translation will require an integrated approach that ensures clinical efficacy, safety, and industrial scalability.

7.2 Prospects for the application of 3D-printed scaffolds in real-patient modeling

With the rapid advancement of personalized medicine, 3D-printed scaffolds have emerged as a promising platform for precise intervention and tissue reconstruction [180]. Recent studies have shown that patient-specific vascular models generated through 3D printing can support preprocedural planning, enabling clinicians to design more accurate interventional strategies and thereby improving procedural precision [181, 182].

Meanwhile, other studies have further explored the application of biomimetic materials in scaffold fabrication. For example, scaffolds constructed from biodegradable polymers have demonstrated synchronized mechanical properties and tissue regeneration rates, potentially reducing the need for re-intervention [183, 184]. These findings indicate that 3D-printed scaffolds not only offer mechanical support but also enable physiological integration with the host environment.

Although personalized structural scaffolds have not yet been widely adopted in routine clinical practice, their continued development offers substantial technological potential for optimizing future precision intervention strategies.

7.3 Development of predictive models combining multi-center omics and longitudinal follow-up

To enhance the individualization and predictive accuracy of interventional strategies, the integration of comprehensive multi-center omics data with clinical follow-up is becoming a cornerstone in research and treatment. Collaborative efforts across institutions have led to the establishment of CA databases incorporating genomic, metabolomic, and radiomic features, which are increasingly used to develop predictive models for event risk assessment [185].

Initial validations show that these models possess high predictive accuracy and robust external generalizability, thereby providing valuable support for patient risk stratification and intervention planning [186]. Moreover, the heterogeneity and scalability of multi-center datasets contribute to enhanced model robustness, adaptability, and long-term stability [187].

Looking ahead, iterative model updates informed by real-time follow-up data will facilitate the dynamic integration of predictive precision and individualized intervention, accelerating the transition of precision intervention from concept to clinical application.

7.4 Prospects of combination therapeutic strategies (e.g., statins/PCSK9i/chimeric antigen receptor T-cell immunotherapy (CAR-T))

In the context of rapidly evolving precision intervention technologies, combining conventional therapies with emerging platforms holds substantial potential. Statins remain a cornerstone in the clinical management of atherosclerotic plaques, and their

integration with nanomedicine platforms has been shown to enhance lipid-lowering effects while improving targeted delivery performance [113].

Some studies suggest that combining PCSK9 inhibitors with targeted nanotherapies enables more effective LDL-C reduction while simultaneously suppressing plaque inflammation. This combinatorial strategy may generate synergistic therapeutic effects through convergent lipid-lowering and immunomodulatory mechanisms [188, 189].

Although CAR-T technology remains at an early stage of investigation in cardiovascular applications, preliminary studies indicate its potential to selectively eliminate pathogenic immune cell subsets. When integrated with localized drug delivery platforms targeting plaques, this approach may offer a powerful synergistic pathway that combines immune remodeling with structural stabilization [190]. However, this strategy demands rigorous risk assessment and safety validation. Bridging the clinical translation gap will require a comprehensive closed-loop system encompassing upstream mechanistic targeting, platform engineering, and AI-assisted strategy optimization, to enhance both scientific rigor and clinical adaptability of engineered interventions (Fig. 8).

7.5 Regulatory and ethical considerations: real-world barriers to precision intervention

As nanoplatforms, 3D-printed scaffolds, and AI systems increasingly converge to enable precision intervention in CA, a series of regulatory and ethical challenges has emerged during clinical translation. These issues warrant early and systematic consideration at the foundational research stage [191, 192].

First, the immunogenicity and systemic toxicity of nanomaterials remain a major barrier in preclinical validation [193–195]. Although many studies have confirmed their favorable biocompatibility and biodegradability, large-scale animal data on batch-to-batch consistency, long-term stability, and interindividual variability are still lacking. These gaps hinder compliance with the stringent release standards required for therapeutic-grade materials by regulatory agencies.

Second, manufacturing consistency and regulatory alignment represent critical translational challenges for the industrialization of 3D-printed scaffolds. While personalized printing offers clear advantages in customization, it also complicates standardization and large-scale reproducibility. This tension necessitates the establishment of a comprehensive standard system encompassing design specifications, printing materials, and post-processing workflows, all subject to dual oversight under GMP (Good Manufacturing Practice) and MDR (Medical Device Regulation).

Even more complex are the issues surrounding the interpretability, safety, and ethical governance of AI systems. Digital twin models require the integration and dynamic analysis of multisource patient data, raising concerns regarding data privacy, algorithmic bias, and model opacity. Accordingly, ethical governance frameworks, including transparency auditing, data anonymization protocols, and informed consent procedures, must be implemented to ensure that AI systems remain traceable, auditable, and reproducible, in compliance with evolving clinical AI regulations (e.g., the EU AI Act and FDA AI/ML guidance draft) [196].

Therefore, as CA precision intervention platforms advance toward clinical application, it is imperative to simultaneously

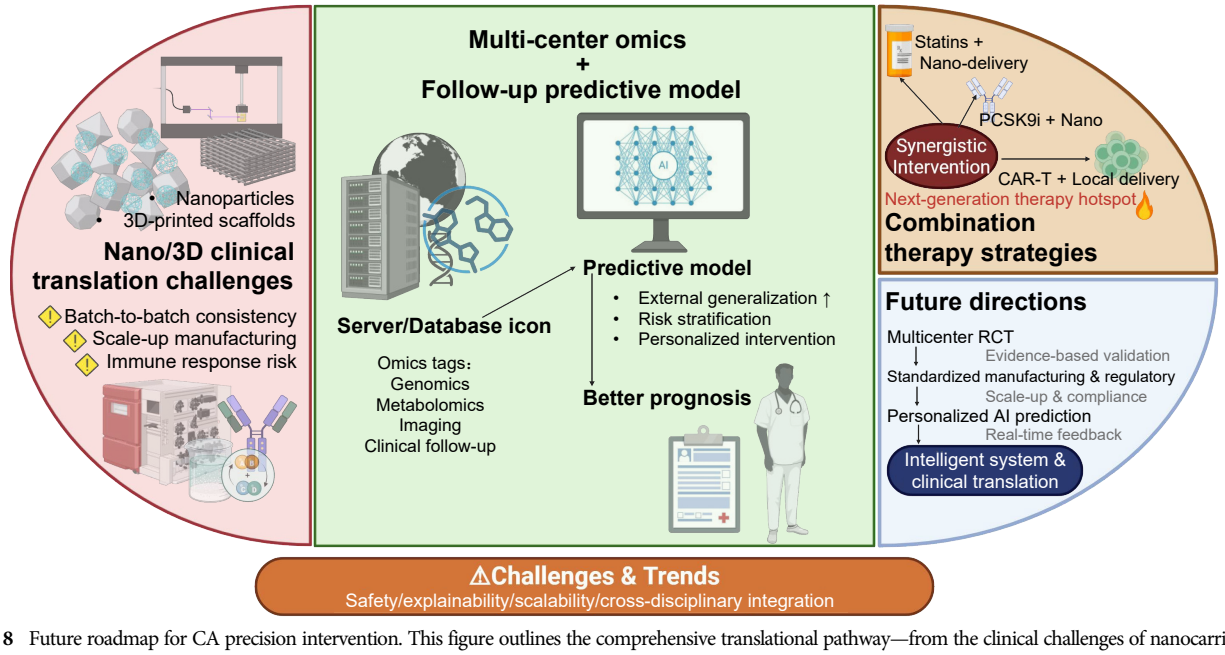

Figure 8 Future roadmap for CA precision intervention. This figure outlines the comprehensive translational pathway—from the clinical challenges of nanocarriers and 3D-printed scaffolds, through multi-center omics-driven predictive modeling, to emerging combination therapies and future intelligent implementation. The left section highlights key hurdles in clinical translation of nanocarriers and 3D-printed scaffolds, including issues of consistency, scalability, and immunogenicity. The center section presents the construction of predictive models integrating multi-center omics and longitudinal follow-up data, incorporating genomics, metabolomics, imaging, and clinical outcomes to enable external generalizability, risk stratification, and personalized intervention, thereby improving prognosis. The upper-right corner summarizes next-generation combination strategies such as "statins + nanocarrier delivery", "PCSK9 inhibitors + nanocarriers", and "CAR-T + localized delivery", representing emerging therapeutic directions. The lower-right section envisions future development, emphasizing the importance of multi-center randomized controlled trials (RCTs), standardized manufacturing and regulatory compliance, scalable and stable engineering platforms, individualized AI-driven prediction, and real-time feedback—ultimately advancing toward intelligent systems and clinical integration. The bottom bar outlines key future challenges and trends, including safety, explainability, scalability, and interdisciplinary integration.

Table 5 A three-dimensional coordinated pathway for precision intervention in coronary atherosclerosis: from spatiotemporal mechanisms to engineering-AI closed loop

Dimension module	Example targets/features	Material/platform design parameters	AI-assisted strategies
Spatiotemporal mechanisms Layer [34, 77]	TREM2$^+$ macrophage clustering (edge); HIF-1α hypoxia-enriched regions; ABCA1 in fibrous caps	Anchored delivery (e.g., VCAM-1 antibody); pH/ROS-responsive modules; fibrous cap-targeted scaffold release	Spatial transcriptomics analysis; tissue atlas modeling; graph neural networks for distribution prediction
Delivery platform layer [137]	siRNA/miR-33a for gene modulation; anti-inflammatory/anti-foam cell drug combinations	Nanoparticle size: 50–150 nm; degradable PLGA with core-shell design; biomimetic porous 3D-printed scaffolds	AI-assisted material selection; release rate-timing optimization; prediction of material-tissue compatibility
Intelligent systems layer [197]	Modeling of metabolic heterogeneity and lesion-hemodynamic coupling	Customized structural-mechanical parameters; automated scaffold printing; prediction of material-cell interactions	Multimodal data integration; digital twin modeling; simulation-guided pathway recommendation

address the threefold foundation of material safety, manufacturing compliance, and algorithmic ethics, ultimately establishing a closed-loop system that integrates technology, regulation, and ethics.

8 Conclusions

CA, characterized by marked heterogeneity and chronic progression, remains a leading cause of cardiovascular morbidity and mortality worldwide. Its pathophysiology extends beyond traditional features such as lipid accumulation and endothelial dysfunction to encompass pronounced spatial heterogeneity in immune microenvironmental imbalance and metabolic reprogramming. This complexity renders treatment strategies based on single biomarkers or discrete pathological stages insufficient for comprehensively addressing high-risk populations, particularly in predicting MI recurrence or asymptomatic plaque rupture. Conventional therapies centered on lipid-lowering or antiplatelet regimens show limited efficacy in certain high-risk cohorts, highlighting the urgent need for more precise intervention targets and delivery platforms.

The systematic design of precision intervention strategies for CA has evolved beyond a unidimensional technological assembly into a coordinated optimization process spanning three axes: "spatiotemporal mechanism decoding", "delivery pathway construction", and "intelligent system feedback". To elucidate the logical flow and engineering correlations among these modules, this review proposes an integrated "three-dimensional matrix", using "mechanism identification-target mapping-material parameters-AI optimization" as the vertical backbone to establish a traceable closed-loop from pathological discovery to intervention design (Table 5 [34, 77, 137, 197]).

Based on a comprehensive review of recent advances in CA research, this study integrates multidisciplinary achievements across multimodal omics, ST analysis, immunometabolic pathway identification, engineered intervention material development, and AI-assisted evaluation. It proposes a four-dimensional coupled model of "mechanism-target-platform-system" for closed-loop intervention. Specifically, multi-omics profiling provides a panoramic view of the plaque microenvironment, and spatial expression heterogeneity of targets such as TREM2, HIF-1α, and ABCA1 offers entry points for immunometabolic intervention. Engineering technologies like nanocarrier drug delivery and 3D-printed scaffolds construct the platforms for targeted delivery and structural support. The integration of AI and digital twin systems further enables individualized intervention pathways to be simulated and iteratively refined. Collectively, this closed-loop framework enhances the specificity and adaptability of intervention design and establishes a conceptual bridge linking mechanistic insight to clinical translation.

The translation of precision intervention strategies for CA from laboratory research to clinical application requires sustained focus on three core directions. First, at the mechanistic level, a deeper elucidation of key regulatory pathways and intercellular interaction networks is needed to construct a systematic map of lesion evolution. Second, at the technological level, emphasis must be placed on standardized modeling, scalable manufacturing, and cross-center reproducibility of engineered platforms. Finally, at the application level, there is a pressing need to establish real-world data cohorts integrating multimodal omics, imaging, intervention, and follow-up, while also exploring interpretability and safety standards for AI-based decision support systems. Only through interdisciplinary collaboration and the coordinated integration of data, platforms, and clinical practice can CA interventions achieve true individualization, adaptability, and long-term clinical impact.

Future research and clinical translation of CA intervention strategies should move beyond isolated breakthroughs in materials or algorithms and instead adopt a systems-engineering paradigm that is mechanism-driven, material-enabled, and intelligence-guided. With the synergistic advancement of omics technologies, programmable biomaterials, and AI-assisted decision-making, a multidimensional and dynamically adjustable intervention framework is gradually emerging. This paradigm offers a promising pathway toward truly personalized therapeutic solutions for CA and other complex chronic diseases.

Data availability

Not applicable.

Acknowledgements

This study was supported by the Foundation of Yangpu District Health Commission (No. YPM202415).

Declaration of competing interest

The authors declare no conflict of interest.

Author contribution statement

M. G. and Y. L. contributed equally to this work. M. G. was responsible for the conceptualization of the review, conducted the investigation, wrote the original draft, and designed the visualization. Y. L. participated in the investigation and data curation, performed the formal analysis, and contributed significantly to the writing of the original draft. R. G. provided

supervision, acquired the funding, administered the project, and was responsible for the writing, review, and editing of the manuscript.

Informed consent

Not applicable.

Ethics statement

Not applicable.

Use of AI statement

None.

References

[1] Banach, M.; Reiner, Ž.; Surma, S.; Bajraktari, G.; Bielecka-Dabrowa, A.; Bunc, M.; Bytyçi, I.; Ceska, R.; Cicero, A. F. G.; Dudek, D. et al. 2024 Recommendations on the optimal use of lipid-lowering therapy in established atherosclerotic cardiovascular disease and following acute coronary syndromes: A position paper of the International Lipid Expert Panel (ILEP). *Drugs* **2024**, *84*, 1541–1577.

[2] Timmis, A.; Vardas, P.; Townsend, N.; Torbica, A.; Katus, H.; De Smedt, D.; Gale, C. P.; Maggioni, A. P.; Petersen, S. E.; Huculeci, R. et al. European Society of Cardiology: Cardiovascular disease statistics 2021. *Eur. Heart J.* **2022**, *43*, 716–799.

[3] Hong, S. J.; Lee, Y. J.; Lee, S. J.; Hong, B. K.; Kang, W. C.; Lee, J. Y.; Lee, J. B.; Yang, T. H.; Yoon, J.; Ahn, C. M. et al. Treat-to-target or high-intensity statin in patients with coronary artery disease. *JAMA* **2023**, *329*, 1078.

[4] Attiq, A.; Afzal, S.; Ahmad, W.; Kandeel, M. Hegemony of inflammation in atherosclerosis and coronary artery disease. *Eur. J. Pharmacol.* **2024**, *966*, 176338.

[5] Chen, R. K.; Zhang, H. R.; Tang, B. T.; Luo, Y. K.; Yang, Y. F.; Zhong, X.; Chen, S. F.; Xu, X. J.; Huang, S. K.; Liu, C. Z. Macrophages in cardiovascular diseases: Molecular mechanisms and therapeutic targets. *Sig. Transduct. Target. Ther.* **2024**, *9*, 130.

[6] Tall, A. R.; Bornfeldt, K. E. Inflammasomes and atherosclerosis: A mixed picture. *Circ. Res.* **2023**, *132*, 1505–1520.

[7] Zhang, S. T.; Lin, H.; Wang, J. L.; Rui, J. Y.; Wang, T. W.; Cai, Z. Y.; Huang, S. M.; Gao, Y. X.; Ma, T. F.; Fan, R. et al. Sensing ceramides by CYSLTR2 and P2RY6 to aggravate atherosclerosis. *Nature* **2025**, *641*, 476–485.

[8] Gastanadui, M. G.; Margaroli, C.; Litovsky, S.; Richter, R. P.; Wang, D. Z.; Xing, D. Q.; Wells, J. M.; Gaggar, A.; Nanda, V.; Patel, R. P. et al. Spatial transcriptomic approach to understanding coronary atherosclerotic plaque stability. *ATVB* **2024**, *44*, e264–e276.

[9] Sun, J. M.; Singh, P.; Shami, A.; Kluza, E.; Pan, M. Y.; Djordjevic, D.; Michaelsen, N. B.; Kennbäck, C.; Van Der Wel, N. N.; Orho-Melander, M. et al. Spatial transcriptional mapping reveals site-specific pathways underlying human atherosclerotic plaque rupture. *J. Am. Coll. Cardiol.* **2023**, *81*, 2213–2227.

[10] Mosquera, J. V.; Auguste, G.; Wong, D.; Turner, A. W.; Hodonsky, C. J.; Alvarez-Yela, A. C.; Song, Y. P.; Cheng, Q.; Lino Cardenas, C. L.; Theofilatos, K. et al. Integrative single-cell meta-analysis reveals disease-relevant vascular cell states and markers in human atherosclerosis. *Cell Rep.* **2023**, *42*, 113380.

[11] Traeuble, K.; Munz, M.; Pauli, J.; Sachs, N.; Vafadarnejad, E.; Carrillo-Roa, T.; Maegdefessel, L.; Kastner, P.; Heinig, M. Integrated single-cell atlas of human atherosclerotic plaques. *Nat. Commun.* **2025**, *16*, 8255.

[12] Xu, M. Z.; Qi, Y. M.; Liu, G. S.; Song, Y. Q.; Jiang, X. Y.; Du, B. J. Size-dependent *in vivo* transport of nanoparticles: Implications for delivery, targeting, and clearance. *ACS Nano* **2023**, *17*, 20825–20849.

[13] Han, X. Y.; Saiding, Q.; Cai, X. L.; Xiao, Y.; Wang, P.; Cai, Z. W.; Gong, X.; Gong, W. M.; Zhang, X. C.; Cui, W. G. Intelligent vascularized 3D/4D/5D/6D-printed tissue scaffolds. *Nano-Micro Lett.* **2023**, *15*, 239.

[14] Gong, X. Y.; Wen, Z.; Liang, Z. X.; Xiao, H.; Lee, S.; Rossello‐Martinez, A.; Xing, Q. Z.; Wright, T.; Nguyen, R. Y.; Mak, M. Instant assembly of collagen for tissue engineering and bioprinting. *Nat. Mater.* **2025**, *24*, 1307–1318.

[15] Muñoz-Hernando, M.; Nogales, P.; Fernández-Barahona, I.; Ruiz-Cabello, J.; Bentzon, J. F.; Herranz, F. Sphingomyelinase-responsive nanomicelles for targeting atherosclerosis. *Nanoscale* **2024**, *16*, 6477–6487.

[16] Straughan, R.; Kadry, K.; Parikh, S. A.; Edelman, E. R.; Nezami, F. R. Fully automated construction of three-dimensional finite element simulations from Optical Coherence Tomography. *Comput. Biol. Med.* **2023**, *165*, 107341.

[17] Lv, J. J.; Wang, H.; Zhang, C.; Zhang, T. J.; Wei, H. L.; Liu, Z. K.; Ma, Y. H.; Yang, Z.; He, Q.; Wang, L. J. et al. CD147 sparks atherosclerosis by driving M1 phenotype and impairing efferocytosis. *Circ. Res.* **2024**, *134*, 165–185

[18] Wu, J. Y.; He, S. P.; Song, Z. K.; Chen, S. K.; Lin, X. F.; Sun, H. M.; Zhou, P. Y.; Peng, Q. B.; Du, S. L.; Zheng, S. Y. et al. Macrophage polarization states in atherosclerosis. *Front. Immunol.* **2023**, *14*, 1185587.

[19] Yang, Y. J.; Bai, D. D.; Jiang, L. H.; Chen, Y. R.; Wang, M. Y.; Wang, W. X.; Wang, H. X.; He, Q. S.; Bu, G. R.; Long, J. et al. Stilbene glycosides alleviate atherosclerosis partly by promoting lipophagy of dendritic cells. *Int. Immunopharmacol.* **2024**, *143*, 113223.

[20] Zhang, Y. J.; Jiang, H.; Dong, M. D.; Min, J.; He, X.; Tan, Y. K.; Liu, F. H.; Chen, M. H.; Chen, X.; Yin, Q. W. et al. Macrophage MCT4 inhibition activates reparative genes and protects from atherosclerosis by histone H3 lysine 18 lactylation. *Cell Rep.* **2024**, *43*, 114180.

[21] Schilperoort, M.; Ngai, D.; Katerelos, M.; Power, D. A.; Tabas, I. PFKFB2-mediated glycolysis promotes lactate-driven continual efferocytosis by macrophages. *Nat. Metab.* **2023**, *5*, 431–444.

[22] Gianopoulos, I.; Daskalopoulou, S. S. Macrophage profiling in atherosclerosis: Understanding the unstable plaque. *Basic Res. Cardiol.* **2024**, *119*, 35–56.

[23] Guo, Z. Y.; Zhang, W.; Gao, H. X.; Li, Y.; Li, X.; Yang, X. H.; Fan, L. H. High expression levels of haem oxygenase-1 promote ferroptosis in macrophage-derived foam cells and exacerbate plaque instability. *Redox Biol.* **2024**, *76*, 103345.

[24] Neels, J. G.; Gollentz, C.; Chinetti, G. Macrophage death in atherosclerosis: Potential role in calcification. *Front. Immunol.* **2023**, *14*, 1215612.

[25] Zheng, S. H.; Que, X. Y.; Wang, S. X.; Zhou, Q.; Xing, X. K.; Chen, L.; Hou, C. Y.; Ma, J. F.; An, P.; Peng, Y. H. et al. ZDHHC5-mediated NLRP3 palmitoylation promotes NLRP3-NEK7 interaction and inflammasome activation. *Mol. Cell* **2023**, *83*, 4570–4585.e7

[26] Pandey, A.; Li, Z. Y.; Gautam, M.; Ghosh, A.; Man, S. M. Molecular mechanisms of emerging inflammasome complexes and their activation and signaling in inflammation and pyroptosis. *Immunol. Rev.* **2025**, *329*, e13406.

[27] Grebe, A.; Hoss, F.; Latz, E. NlRP3 inflammasome and the IL-1 pathway in atherosclerosis. *Circ. Res.* **2018**, *122*, 1722–1740

[28] Forsythe, J. A.; Jiang, B. H.; Iyer, N. V.; Agani, F.; Leung, S. W.; Koos, R. D.; Semenza, G. L. Activation of vascular endothelial growth factor gene transcription by hypoxia-inducible factor 1. *Mol. Cell. Biol.* **1996**, *16*, 4604–4613.

[29] Akhter, N.; Wilson, A.; Arefanian, H.; Thomas, R.; Kochumon, S.; Al-Rashed, F.; Abu-Farha, M.; Al-Madhoun, A.; Al-Mulla, F.; Ahmad, R. et al. Endoplasmic reticulum stress promotes the expression of TNF-α in THP-1 cells by mechanisms involving ROS/CHOP/HIF-1α and MAPK/NF-κB pathways. *IJMS* **2023**, *24*, 15186.

[30] Singh, A.; Schurman, S. H.; Bektas, A.; Kaileh, M.; Roy, R.; Wilson, D. M.; Sen, R.; Ferrucci, L. Aging and inflammation. *Cold Spring Harb. Perspect. Med.* **2024**, *14*, a041197.

[31] Cheng, C.; Zhang, J.; Li, X. D.; Xue, F.; Cao, L.; Meng, L. L.; Sui, W.; Zhang, M.; Zhao, Y. X.; Xi, B. et al. NPRC deletion mitigated atherosclerosis by inhibiting oxidative stress, inflammation and apoptosis in ApoE knockout mice. *Sig. Transduct. Target. Ther.* **2023**, *8*, 290.

[32] Greco, F.; Bertagna, G.; Quercioli, L.; Pucci, A.; Rocchiccioli, S.; Ferrari, M.; Recchia, F. A.; Mcdonnell, L. A. Lipids associated with atherosclerotic plaque instability revealed by mass spectrometry imaging of human carotid arteries. *Atherosclerosis* **2024**, *397*, 118555.

[33] Winkels, H.; Wolf, D. Heterogeneity of T cells in atherosclerosis defined by single-cell RNA-sequencing and cytometry by time of flight. *ATVB* **2021**, *41*, 549–563.

[34] Kheirolomoom, A.; Kim, C. W.; Seo, J. W.; Kumar, S.; Son, D. J.; Gagnon, M. K. J.; Ingham, E. S.; Ferrara, K. W.; Jo, H. Multifunctional nanoparticles facilitate molecular targeting and miRNA delivery to inhibit atherosclerosis in ApoE$^{-/-}$ mice. *ACS Nano* **2015**, *9*, 8885–8897.

[35] Li, J. W.; Li, X. Y.; Song, S. J.; Sun, Z. W.; Li, Y. Z.; Yang, L.; Xie, Z. H.; Cai, Y. K.; Zhao, Y. P. Mitochondria spatially and temporally modulate VSMC phenotypes via interacting with cytoskeleton in cardiovascular diseases. *Redox Biol.* **2023**, *64*, 102778.

[36] Bao, Q. K.; Zhang, B. Y.; Zhou, L.; Yang, Q.; Mu, X. F.; Liu, X.; Zhang, S. Y.; Yuan, M.; Zhang, Y.; Che, J. J. et al. CNP ameliorates macrophage inflammatory response and atherosclerosis. *Circ. Res.* **2024**, *134*, e72–e91.

[37] Patterson, M. T.; Firulyova, M. M.; Xu, Y. Z.; Hillman, H.; Bishop, C.; Zhu, A. L. S.; Hickok, G. H.; Schrank, P. R.; Ronayne, C. E.; Caillot, Z. et al. Trem2 promotes foamy macrophage lipid uptake and survival in atherosclerosis. *Nat. Cardiovasc. Res.* **2023**, *2*, 1015–1031.

[38] Hou, P. B.; Fang, J. K.; Liu, Z. H.; Shi, Y. F.; Agostini, M.; Bernassola, F.; Bove, P.; Candi, E.; Rovella, V.; Sica, G. et al. Macrophage polarization and metabolism in atherosclerosis. *Cell Death Dis.* **2023**, *14*, 691.

[39] Wang, Q.; Wang, Y. R.; Xu, D. Y. Research progress on Th17 and T regulatory cells and their cytokines in regulating atherosclerosis. *Front. Cardiovasc. Med.* **2022**, *9*, 929078.

[40] Chang, S. Y.; Wang, Z. H.; An, T. H. T-cell metabolic reprogramming in atherosclerosis. *Biomedicines* **2024**, *12*, 1844.

[41] Li, L. F.; Wang, M.; Ma, Q. X.; Ye, J. X.; Sun, G. B. Role of glycolysis in the development of atherosclerosis. *Am. J. Physiol.-Cell Physiol.* **2022**, *323*, C617–C629.

[42] Duewell, P.; Kono, H.; Rayner, K. J.; Sirois, C. M.; Vladimer, G.; Bauernfeind, F. G.; Abela, G. S.; Franchi, L.; Nuñez, G.; Schnurr, M. et al. NLRP3 inflammasomes are required for atherogenesis and activated by cholesterol crystals. *Nature* **2010**, *464*, 1357–1361

[43] Galkina, E.; Ley, K. Vascular adhesion molecules in atherosclerosis. *ATVB* **2007**, *27*, 2292–2301.

[44] Sharma, M.; Schlegel, M. P.; Afonso, M. S.; Brown, E. J.; Rahman, K.; Weinstock, A.; Sansbury, B. E.; Corr, E. M.; Van Solingen, C.; Koelwyn, G. J. et al. Regulatory T cells license macrophage pro-resolving functions during atherosclerosis regression. *Circ. Res.* **2020**, *127*, 335–353.

[45] Taleb, S.; Tedgui, A.; Mallat, Z. IL-17 and Th17 cells in atherosclerosis. *ATVB* **2015**, *35*, 258–264.

[46] Teigen, M.; Ølnes, Å. S.; Bjune, K.; Leren, T. P.; Bogsrud, M. P.; Strøm, T. B. Functional characterization of missense variants affecting the extracellular domains of ABCA1 using a fluorescence-based assay. *J. Lipid Res.* **2024**, *65*, 100482.

[47] Chen, Y. Y.; Cui, Y. T.; Li, M.; Xia, M. D.; Xiang, Q.; Mao, Y.; Li, H. J.; Chen, J. L.; Zeng, W.; Zheng, X. L. et al. A novel mechanism of ferroptosis inhibition - enhanced atherosclerotic plaque stability: YAP1 suppresses vascular smooth muscle cell ferroptosis through GLS1. *FASEB J.* **2024**, *38*, e23850.

[48] Zhao, Y. C.; Xiong, W. D.; Li, C. F.; Zhao, R. Z.; Lu, H.; Song, S.; Zhou, Y.; Hu, Y. Q.; Shi, B.; Ge, J. B. Hypoxia-induced signaling in the cardiovascular system: Pathogenesis and therapeutic targets. *Sig. Transduct. Target. Ther.* **2023**, *8*, 431.

[49] Miano, J. M.; Fisher, E. A.; Majesky, M. W. Fate and state of vascular smooth muscle cells in atherosclerosis. *Circulation* **2021**, *143*, 2110–2116.

[50] Ye, W. J.; Chen, Z. B.; Xia, Z. W.; Li, D. J. Single-cell RNA sequencing in human atherosclerotic plaques reveals a novel smooth muscle cell subtype that possesses multi differentiation potential and shapes the microenvironment. *Clin. Exp. Med.* **2025**, *25*, 251.

[51] Liu, C.; Yang, F.; Su, X.; Zhang, Z. P.; Xing, Y. W. ScRNA-seq and spatial transcriptomics: Exploring the occurrence and treatment of coronary-related diseases starting from development. *Front. Cardiovasc. Med.* **2023**, *10*, 1064949.

[52] Han, S. J.; Xu, Q. Q.; Du, Y. W.; Tang, C. W.; Cui, H. R.; Xia, X. F.; Zheng, R.; Sun, Y.; Shang, H. C. Single-cell spatial transcriptomics in cardiovascular development, disease, and medicine. *Genes Dis.* **2024**, *11*, 101163.

[53] Campos, J.; McMurray, J. L.; Certo, M.; Hardikar, K.; Morse, C.; Corfield, C.; Weigand, B. M.; Yang, K.; Shoaran, M.; Otto, T. D. et al. Spatial transcriptomics elucidates localized immune responses in atherosclerotic coronary artery. *EMBO Mol. Med.* **2025**, *17*, 2827–2846.

[54] Pepin, M. E.; Schwartzman, W. E.; Fang, S.; Vellarikkal, S. K.; Atri, D. S.; Reddy, A.; Xu, Q. H.; Hamel, A. R.; Billaud, M.; Segrè, A. V. et al. Integrative analysis of single-cell transcriptomics and genetic associations identify cell states associated with vascular disease. *Atherosclerosis* **2025**, *403*, 119108.

[55] Jin, W.; Ma, J. C.; Rong, L.; Huang, S. S.; Li, T.; Jin, G. X.; Zhou, Z. J. Semi-automated IT-scATAC-seq profiles cell-specific chromatin accessibility in differentiation and peripheral blood populations. *Nat. Commun.* **2025**, *16*, 2635.

[56] Hou, X. H.; Li, Z. P.; Lin, J.; Lin, W.; Li, L. Y.; Zheng, X. Q.; Lai, X. L.; Zhu, L.; Guo, P. F.; Cai, F. G. et al. Single-cell transcriptome integrated with genome-wide association study reveals heterogeneity of carotid and femoral plaques and its association with plaque stability. *Sci. Rep.* **2025**, *15*, 11812.

[57] Örd, T.; Lönnberg, T.; Nurminen, V.; Ravindran, A.; Niskanen, H.; Kiema, M.; Õunap, K.; Maria, M.; Moreau, P. R.; Mishra, P. P. et al. Dissecting the polygenic basis of atherosclerosis via disease-associated cell state signatures. *Am. J. Human Genet.* **2023**, *110*, 722–740.

[58] Lambert, J.; Oc, S.; Worssam, M. D.; Häußler, D.; Solomon, C. U.; Figg, N. L.; Baxter, R.; Imaz, M.; Taylor, J. C. K.; Foote, K. et al. Network-based prioritization and validation of regulators of vascular smooth muscle cell proliferation in disease. *Nat. Cardiovasc. Res.* **2024**, *3*, 714–733.

[59] Luo, Y. T.; Luo, J. J.; An, P.; Zhao, Y. F.; Zhao, W. T.; Fang, Z.; Xia, Y.; Zhu, L.; Xu, T.; Zhang, X. et al. The activator protein-1 complex governs a vascular degenerative transcriptional programme in smooth muscle cells to trigger aortic dissection and rupture. *Eur. Heart J.* **2024**, *45*, 287–305.

[60] Mocci, G.; Sukhavasi, K.; Örd, T.; Bankier, S.; Singha, P.; Arasu, U. T.; Agbabiaje, O. O.; Mäkinen, P.; Ma, L. J.; Hodonsky, C. J. et al. Single-cell gene-regulatory networks of advanced symptomatic atherosclerosis. *Circ. Res.* **2024**, *134*, 1405–1423.

[61] Jiang, K. S.; He, Y.; Hu, B. J.; Quan, L.; Peng, L. Y.; Tian, J. T.;

Zhou, N.; Huang, E. W.; Zhao, Q. H. Identification of pyroptosis related genes and subtypes in atherosclerosis using multiomic and single cell analysis. *Sci. Rep.* **2025**, *15*, 22360.

[62] Qin, X. H.; Ding, R.; Lu, H. R.; Zhang, W. F.; Wei, S. S.; Ji, B. W.; Geng, R. X.; Wu, L. Q.; Chen, Z. B. Identification of pivotal genes and regulatory networks associated with atherosclerotic carotid artery stenosis based on comprehensive bioinformatics analysis and machine learning. *Front. Pharmacol.* **2024**, *15*, 1364160.

[63] Jin, S. Q.; Plikus, M. V.; Nie, Q. CellChat for systematic analysis of cell-cell communication from single-cell transcriptomics. *Nat. Protoc.* **2025**, *20*, 180–219.

[64] Wu, Y. F.; Chang, N. W.; Chu, L. A.; Liu, H. Y.; Zhou, Y. X.; Pai, Y. L.; Yu, Y. S.; Kuan, C. H.; Wu, Y. C.; Lin, S. J. et al. Single-cell transcriptomics reveals cellular heterogeneity and complex cell-cell communication networks in the mouse cornea. *Invest. Ophthalmol. Vis. Sci.* **2023**, *64*, 5.

[65] Li, Y.; Wang, S. S.; Zhang, R. D.; Gong, Y. Y.; Che, Y. L.; Li, K. N.; Pan, Z. F. Single-cell and spatial analysis reveals the interaction between ITLN1$^+$ foam cells and SPP1$^+$ macrophages in atherosclerosis. *Front. Cardiovasc. Med.* **2025**, *12*, 1510082.

[66] Bashore, A. C.; Yan, H. Y.; Xue, C. Y.; Zhu, L. Y.; Kim, E.; Mawson, T.; Coronel, J.; Chung, A.; Sachs, N.; Ho, S. et al. High-dimensional single-cell multimodal landscape of human carotid atherosclerosis. *ATVB* **2024**, *44*, 930–945.

[67] Örd, T.; Õunap, K.; Stolze, L. K.; Aherrahrou, R.; Nurminen, V.; Toropainen, A.; Selvarajan, I.; Lönnberg, T.; Aavik, E.; Ylä-Herttuala, S. et al. Single-cell epigenomics and functional fine-mapping of atherosclerosis GWAS loci. *Circ. Res.* **2021**, *129*, 240–258.

[68] Qian, Q. H.; Xue, R. K.; Xu, C. L.; Wang, F. Y.; Zeng, J. Y.; Xiao, J. F. CVD Atlas: A multi-omics database of cardiovascular disease. *Nucl. Acids Res.* **2025**, *53*, D1348–D1355.

[69] Zernecke, A.; Erhard, F.; Weinberger, T.; Schulz, C.; Ley, K.; Saliba, A. E.; Cochain, C. Integrated single-cell analysis-based classification of vascular mononuclear phagocytes in mouse and human atherosclerosis. *Cardiovasc. Res.* **2023**, *119*, 1676–1689.

[70] Tamargo, I. A.; Baek, K. I.; Xu, C. B.; Kang, D. W.; Kim, Y.; Andueza, A.; Williams, D.; Demos, C.; Villa-Roel, N.; Kumar, S. et al. HEG1 protects against atherosclerosis by regulating stable flow-induced KLF2/4 expression in endothelial cells. *Circulation* **2024**, *149*, 1183–1201

[71] Fu, J. N.; Wu, H. Structural mechanisms of NLRP3 inflammasome assembly and activation. *Annu. Rev. Immunol.* **2023**, *41*, 301–316.

[72] Paramel Varghese, G.; Folkersen, L.; Strawbridge, R. J.; Halvorsen, B.; Yndestad, A.; Ranheim, T.; Krohg‐Sørensen, K.; Skjelland, M.; Espevik, T.; Aukrust, P. et al. NLRP3 inflammasome expression and activation in human atherosclerosis. *JAHA* **2016**, *5*, e003031

[73] Jin, Y.; Fu, J. Novel insights into the NLRP3 inflammasome in atherosclerosis. *JAHA* **2019**, *8*, e012219.

[74] Xu, R. H.; Yuan, W.; Wang, Z. Q. Advances in glycolysis metabolism of atherosclerosis. *J. Cardiovasc. Trans. Res.* **2023**, *16*, 476–490.

[75] Dudley, A. C.; Griffioen, A. W. Pathological angiogenesis: Mechanisms and therapeutic strategies. *Angiogenesis* **2023**, *26*, 313–347.

[76] Cyréus, P.; Wadén, K.; Hellberg, S.; Bergman, O.; Lengquist, M.; Karlöf, E.; Buckler, A.; Matic, L.; Roy, J.; Marlevi, D. et al. Atherosclerotic plaque instability in symptomatic non-significant carotid stenoses. *JVS-Vasc. Sci.* **2025**, *6*, 100280.

[77] Piollet, M.; Porsch, F.; Rizzo, G.; Kapser, F.; Schulz, D. J. J.; Kiss, M. G.; Schlepckow, K.; Morenas-Rodriguez, E.; Sen, M. O.; Gropper, J. et al. TREM2 protects from atherosclerosis by limiting necrotic core formation. *Nat. Cardiovasc. Res.* **2024**, *3*, 269–282.

[78] Peng, X.; Sun, B.; Tang, C. H.; Shi, C. Y.; Xie, X. W.; Wang, X. Y.; Jiang, D. S.; Li, S.; Jia, Y.; Wang, Y. N. et al. HMOX1-LDHB interaction promotes ferroptosis by inducing mitochondrial dysfunction in foamy macrophages during advanced atherosclerosis. *Dev. Cell* **2025**, *60*, 1070–1086.e8

[79] Zhu, B. T.; Liu, Y. X.; Peng, D. Q. The double-edged role and therapeutic potential of TREM2 in atherosclerosis. *Biomark. Res.* **2024**, *12*, 131.

[80] Fabre, T.; Barron, A. M. S.; Christensen, S. M.; Asano, S.; Bound, K.; Lech, M. P.; Wadsworth, M. H.; Chen, X.; Wang, C.; Wang, J. et al. Identification of a broadly fibrogenic macrophage subset induced by type 3 inflammation. *Sci. Immunol.* **2023**, *8*, eadd8945.

[81] Zhang, M.; Hou, L. J.; Tang, W. Y.; Lei, W. X.; Lin, H. L.; Wang, Y.; Long, H. J.; Lin, S. Y.; Chen, Z.; Wang, G. L. et al. Oridonin attenuates atherosclerosis by inhibiting foam macrophage formation and inflammation through FABP4/PPARγ signalling. *J. Cell. Mol. Med.* **2023**, *27*, 4155–4170.

[82] Jiang, Y.; Yu, M.; Song, Z. F.; Wei, Z. Y.; Huang, J.; Qian, H. Y. Targeted delivery of mesenchymal stem cell-derived bioinspired exosome-mimetic nanovesicles with platelet membrane fusion for atherosclerotic treatment. *IJN* **2024**, *19*, 2553–2571.

[83] Li, Y.; Pan, J. X.; Yu, J. J. J.; Wu, X. Z.; Yang, G. L.; Pan, X.; Sui, G.; Wang, M. Y.; Cheng, M. J.; Zhu, S. et al. Huayu Qutan Recipe promotes lipophagy and cholesterol efflux through the mTORC1/TFEB/ABCA1‐SCARB1 signal axis. *J. Cell. Mol. Med.* **2024**, *28*, e18257.

[84] Hong, N. E.; Ravodina, A. M.; Asase, C.; Gao, H. Y.; Cherepanova, O. A.; Maiseyeu, A. Itaconate alleviates cholesterol burden via ABCA1 stabilization and cholesterol efflux. *Atherosclerosis* **2025**, *408*, 120445.

[85] Chen, C. Y.; Wang, J.; Pan, D. H.; Wang, X. Y.; Xu, Y. P.; Yan, J. J.; Wang, L. Z.; Yang, X. F.; Yang, M.; Liu, G. P. Applications of multi‐omics analysis in human diseases. *MedComm* **2023**, *4*, e315.

[86] Liu, X. J.; Peng, T.; Xu, M. C.; Lin, S. T.; Hu, B.; Chu, T.; Liu, B. H.; Xu, Y. S.; Ding, W. C.; Li, L. et al. Spatial multi-omics: Deciphering technological landscape of integration of multi-omics and its applications. *J. Hematol. Oncol.* **2024**, *17*, 72.

[87] Zhang, L. R.; Xu, J. L.; Zhou, S. Q.; Yao, F. F.; Zhang, R. Z.; You, W. H.; Dai, J. J.; Yu, K.; Zhang, Y.; Baheti, T. et al. Endothelial DGKG promotes tumor angiogenesis and immune evasion in hepatocellular carcinoma. *J. Hepatol.* **2024**, *80*, 82–98.

[88] Shi, Z. M.; Jing, J. J.; Xue, Z. J.; Chen, W. J.; Tang, Y. B.; Chen, D. J.; Qi, X. Y.; Huang, L.; Zou, Y. Q.; Wu, X. Z. et al. Stellate ganglion block ameliorated central post-stroke pain with comorbid anxiety and depression through inhibiting HIF-1α/NLRP3 signaling following thalamic hemorrhagic stroke. *J. Neuroinflammation* **2023**, *20*, 82.

[89] Li, H. Y.; Liu, P. Y.; Zhang, B.; Yuan, Z. Q.; Guo, M. D.; Zou, X. X.; Qian, Y.; Deng, S. J.; Zhu, L. W.; Cao, X. et al. Acute ischemia induces spatially and transcriptionally distinct microglial subclusters. *Genome Med.* **2023**, *15*, 109.

[90] Xu, S. T.; Yang, B.; Yu, W. H.; Gao, Y.; Cai, H. H.; Wang, Z. Q. TREM2 as a therapeutic target in atherosclerosis. *Cell Biol. Int.* **2025**, *49*, 305–316.

[91] Meng, X. Y.; Asadi-Asadabad, S.; Cao, S.; Song, R.; Lin, Z.; Safhi, M.; Qin, Y.; Tcheumi Tactoum, E.; Taudte, V.; Ekici, A. et al. Metabolic rewiring controlled by HIF-1α tunes IgA-producing B-cell differentiation and intestinal inflammation. *Cell. Mol. Immunol.* **2024**, *22*, 54–67.

[92] Kuzuoglu-Ozturk, D.; Nguyen, H. G.; Xue, L. R.; Figueredo, E.; Subramanyam, V.; Liu, I.; Bonitto, K.; Noronha, A.; Dabrowska, A.; Cowan, J. E. et al. Small-molecule RNA therapeutics to target prostate cancer. *Cancer Cell* **2025**, *43*, 841–855.e8.

[93] Fontana, F.; Giannitti, G.; Marchesi, S.; Limonta, P. The PI3K/Akt pathway and glucose metabolism: A dangerous liaison in cancer. *Int. J. Biol. Sci.* **2024**, *20*, 3113–3125.

[94] Chen, Y.; Ye, X. Y.; Escames, G.; Lei, W. R.; Zhang, X.; Li, M.; Jing, T.; Yao, Y.; Qiu, Z. Y.; Wang, Z. et al. The NLRP3 inflammasome: Contributions to inflammation-related diseases. *Cell. Mol. Biol. Lett.* **2023**, *28*, 51.

[95] Dunsmore, G.; Guo, W.; Li, Z. Y.; Bejarano, D. A.; Pai, R.; Yang, K.; Kwok, I.; Tan, L.; Ng, M.; De La Calle Fabregat, C. et al. Timing and location dictate monocyte fate and their transition to tumor-associated macrophages. *Sci. Immunol.* **2024**, *9*, eadk3981.
[96] Villa-Roel, N.; Ryu, K.; Gu, L. N.; Fernandez Esmerats, J.; Kang, D. W.; Kumar, S.; Jo, H. Hypoxia inducible factor 1α inhibitor PX-478 reduces atherosclerosis in mice. *Atherosclerosis* **2022**, *344*, 20–30.
[97] Chen, Y. G.; Zhang, X. J.; Huang, S. B.; Febbraio, M. Hidden features: CD36/SR-B2, a master regulator of macrophage phenotype/function through metabolism. *Front. Immunol.* **2024**, *15*, 1468957.
[98] Brunham, L. R.; Singaraja, R. R.; Duong, M.; Timmins, J. M.; Fievet, C.; Bissada, N.; Kang, M. H.; Samra, A.; Fruchart, J. C.; Mcmanus, B. et al. Tissue-specific roles of ABCA1 influence susceptibility to atherosclerosis. *ATVB* **2009**, *29*, 548–554.
[99] Castro, R.; Adair, J. H.; Mastro, A. M.; Neuberger, T.; Matters, G. L. VCAM-1-targeted nanoparticles to diagnose, monitor and treat atherosclerosis. *Nanomedicine (Lond)* **2024**, *19*, 723–735.
[100] Wen, S. Y.; Zhi, X. Y.; Liu, H. X.; Wang, X. H.; Chen, Y. Y.; Wang, L. Is the suppression of CD36 a promising way for atherosclerosis therapy. *Biochem. Pharmacol.* **2024**, *219*, 115965.
[101] Ridker, P. M.; Devalaraja, M.; Baeres, F. M. M.; Engelmann, M. D. M.; Hovingh, G. K.; Ivkovic, M.; Lo, L.; Kling, D.; Pergola, P.; Raj, D. et al. IL-6 inhibition with ziltivekimab in patients at high atherosclerotic risk (RESCUE): A double-blind, randomised, placebo-controlled, phase 2 trial. *Lancet* **2021**, *397*, 2060–2069.
[102] Sato, T.; Takeda, N. The roles of HIF-1α signaling in cardiovascular diseases. *J. Cardiol.* **2023**, *81*, 202–208.
[103] Lu, N.; Cheng, W. J.; Liu, D. L.; Liu, G.; Cui, C.; Feng, C. L.; Wang, X. W. NLRP3-mediated inflammation in atherosclerosis and associated therapeutics. *Front. Cell Dev. Biol.* **2022**, *10*, 823387.
[104] Kim, J.; Kim, H. S.; Chung, J. H. Molecular mechanisms of mitochondrial DNA release and activation of the cGAS-STING pathway. *Exp. Mol. Med.* **2023**, *55*, 510–519.
[105] Wang, Y. N.; Chen, L. Q.; Zhang, M. J.; Li, X.; Yang, X. Y.; Huang, T.; Ban, Y. T.; Li, Y. Q.; Li, Q. F.; Zheng, Y. et al. Exercise-induced endothelial Mecp2 lactylation suppresses atherosclerosis via the Ereg/MAPK signalling pathway. *Atherosclerosis* **2023**, *375*, 45–58.
[106] Xiang, P.; Chen, Q. Q.; Chen, L.; Lei, J.; Yuan, Z. Y.; Hu, H.; Lu, Y. N.; Wang, X. M.; Wang, T. T.; Yu, R. H. et al. Metabolite Neu5Ac triggers SLC3A2 degradation promoting vascular endothelial ferroptosis and aggravates atherosclerosis progression in ApoE$^{-/-}$ mice. *Theranostics* **2023**, *13*, 4993–5016.
[107] Huerta, C. T.; Zhang, L. M.; Ortiz, Y. Y.; Li, Y.; Zeynaloo, E.; Dikici, E.; Siahaan, T. J.; Deo, S. K.; Daunert, S.; Liu, Z. J. et al. Directing cell delivery to murine atherosclerotic aortic lesions via targeting inflamed circulatory interface using nanocarriers. *Front. Cardiovasc. Med.* **2025**, *12*, 1517320.
[108] Liu, M. M.; Wang, D. N.; Qi, C. Y.; Zou, M.; Song, J. W.; Li, L. L.; Xie, H. C.; Ren, H. L.; Hao, H. Y.; Yang, G. L. et al. Brain ischemia causes systemic Notch1 activity in endothelial cells to drive atherosclerosis. *Immunity* **2024**, *57*, 2157–2172.e7.
[109] Tang, J.; Li, T.; Xiong, X. J.; Yang, Q. Y.; Su, Z. D. Z.; Zheng, M. M.; Chen, Q. W. Colchicine delivered by a novel nanoparticle platform alleviates atherosclerosis by targeted inhibition of NF-κB/NLRP3 pathways in inflammatory endothelial cells. *J. Nanobiotechnol.* **2023**, *21*, 460.
[110] Li, M.; Zhang, Y. N.; Xiang, K.; Su, Z. K.; Li, X. Y.; Song, H. Y.; Wu, X. H.; Mo, D. Q.; Ren, M. X.; Yang, S. Ant colony-inspired adaptive peptide nanoregulators remodeling the endothelial barrier to alleviate inflammatory responses. *ACS Nano* **2025**, *19*, 16829–16849.
[111] Huang, H. C.; Wang, T. Y.; Rousseau, J.; Orlando, M.; Mungaray, M.; Michaud, C.; Plaisier, C.; Chen, Z. B.; Wang, K. C. Biomimetic nanodrug targets inflammation and suppresses YAP/TAZ to ameliorate atherosclerosis. *Biomaterials* **2024**, *306*, 122505.
[112] Beach, M. A.; Nayanathara, U.; Gao, Y. T.; Zhang, C. H.; Xiong, Y. J.; Wang, Y. F.; Such, G. K. Polymeric nanoparticles for drug delivery. *Chem. Rev.* **2024**, *124*, 5505–5616.
[113] Nenna, A.; Nappi, F.; Larobina, D.; Verghi, E.; Chello, M.; Ambrosio, L. Polymers and nanoparticles for statin delivery: Current use and future perspectives in cardiovascular disease. *Polymers* **2021**, *13*, 711.
[114] Tapio, K.; Mostafa, A.; Kanehira, Y.; Suma, A.; Dutta, A.; Bald, I. A versatile DNA origami-based plasmonic nanoantenna for label-free single-molecule surface-enhanced Raman spectroscopy. *ACS Nano* **2021**, *15*, 7065–7077.
[115] Ferrante, E. A.; Pickard, J. E.; Rychak, J.; Klibanov, A.; Ley, K. Dual targeting improves microbubble contrast agent adhesion to VCAM-1 and P-selectin under flow. *J. Controlled Release* **2009**, *140*, 100–107.
[116] Yang, C.; Mo, L. Q.; Zhang, G. Z.; Dai, Y. X.; Li, B. X.; Tan, Z. H.; Guo, Y. J.; Lu, S.; Hong, Y.; He, H. L. et al. Advancements in dual-targeting nanoparticle strategies for enhanced atherosclerosis therapy: Overcoming limitations of single-targeting approaches. *Bioact. Mater.* **2026**, *55*, 302–333.
[117] Tao, Y.; Lan, X. M.; Zhang, Y.; Fu, C. X.; Liu, L.; Cao, F.; Guo, W. S. Biomimetic nanomedicines for precise atherosclerosis theranostics. *Acta Pharm. Sin. B* **2023**, *13*, 4442–4460.
[118] He, Z. S.; Chen, W.; Hu, K.; Luo, Y. Y.; Zeng, W. Q.; He, X.; Li, T. T.; Ouyang, J.; Li, Y. J.; Xie, L. et al. Resolvin D1 delivery to lesional macrophages using antioxidative black phosphorus nanosheets for atherosclerosis treatment. *Nat. Nanotechnol.* **2024**, *19*, 1386–1398.
[119] Zhu, L.; Zhong, Y.; Yan, M.; Ni, S.; Zhao, X.; Wu, S.; Wang, G. X.; Zhang, K.; Chi, Q. J.; Qin, X. et al. Macrophage membrane-encapsulated dopamine-modified poly cyclodextrin multifunctional biomimetic nanoparticles for atherosclerosis therapy. *ACS Appl. Mater. Interfaces* **2024**, *16*, 32027–32044.
[120] Zhang, X. B.; Rotllan, N.; Canfrán-Duque, A.; Sun, J.; Toczek, J.; Moshnikova, A.; Malik, S.; Price, N. L.; Araldi, E.; Zhong, W. et al. Targeted suppression of miRNA-33 using pHLIP improves atherosclerosis regression. *Circ. Res.* **2022**, *131*, 77–90.
[121] Zhao, G.; Xue, L. L.; Geisler, H. C.; Xu, J. C.; Li, X. Y.; Mitchell, M. J.; Vaughan, A. E. Precision treatment of viral pneumonia through macrophage-targeted lipid nanoparticle delivery. *Proc. Natl. Acad. Sci. USA* **2024**, *121*, e2314747121.
[122] Liu, M. Y.; Ren, Y.; Zhou, Z. J.; Yang, J. X.; Shi, X. H.; Cai, Y.; Arreola, A. X.; Luo, W. Y.; Fung, K. M.; Xu, C. et al. The crosstalk between macrophages and cancer cells potentiates pancreatic cancer cachexia. *Cancer Cell* **2024**, *42*, 885–903.e4.
[123] Wang, L. P.; Wang, W. B.; Wang, Y. F.; Tao, W. L.; Hou, T. X.; Cai, D. F.; Liu, L. K.; Liu, C.; Jiang, K.; Lin, J. Y. et al. The graphene quantum dots gated nanoplatform for photothermal-enhanced synergetic tumor therapy. *Molecules* **2024**, *29*, 615.
[124] Wiraja, C.; Mathiyazhakan, M.; Movahedi, F.; Upputuri, P. K.; Cheng, Y. Y.; Pramanik, M.; Yang, L.; Becker, D. L.; Xu, C. J. Near-infrared light-sensitive liposomes for enhanced plasmid DNA transfection. *Bioeng. Transl. Med.* **2016**, *1*, 357–364.
[125] Teimouri, K.; Ghafari, A.; Kim, M.; Reza Tavakoli, M.; Kim, K. C. Targeted delivery of therapeutic agents in a healthy and stenosed patient-specific carotid artery using an external magnetic field. *J. Magn. Magn. Mater.* **2023**, *585*, 171144.
[126] Gao, W.; Yu, X. Y.; Zhang, C. P.; Du, H. Y.; Yang, S. Y.; Wang, H.; Zhu, J. X.; Luo, Y. K.; Zhang, M. J. Facile fabrications of poly (acrylic acid)-mesoporous zinc phosphate/polydopamine Janus nanoparticles as a biosafe photothermal therapy agent and a pH/NIR-responsive drug carrier. *Acta Biomater.* **2024**, *187*, 328–339.
[127] Villa, C.; Secchi, V.; Macchi, M.; Tripodi, L.; Trombetta, E.; Zambroni, D.; Padelli, F.; Mauri, M.; Molinaro, M.; Oddone, R. et

al. Magnetic-field-driven targeting of exosomes modulates immune and metabolic changes in dystrophic muscle. *Nat. Nanotechnol.* **2024**, *19*, 1532–1543.

[128] Shahverdi, M.; Shaygani, H.; Soltani, M.; Dadkhah, K.; Rezaei Demneh, S. M. H.; Mohammadi, K.; Shamloo, A. Fabrication of a low-kink-radius bilayer vascular scaffold incorporating a TPU stent fabricated via melt electrowriting and an electrospun PCL/PU/gelatin layer. *Sci. Rep.* **2025**, *15*, 24894.

[129] Jiang, W. B.; Zhan, Y. C.; Zhang, Y. F.; Sun, D.; Zhang, G.; Wang, Z. X.; Chen, L. F.; Sun, J. M. Synergistic large segmental bone repair by 3D printed bionic scaffolds and engineered ADSC nanovesicles: Towards an optimized regenerative microenvironment. *Biomaterials* **2024**, *308*, 122566.

[130] Tomić, S. L.; Babić Radić, M. M.; Vuković, J. S.; Filipović, V. V.; Nikodinovic-Runic, J.; Vukomanović, M. Alginate-based hydrogels and scaffolds for biomedical applications. *Mar. Drugs* **2023**, *21*, 177.

[131] Elsayed, E. W.; El-Ashmawy, A. A.; El-Bassyouni, G. T.; Mousa, S. M.; El-Manawaty, M.; Emara, L. H. Formulation and evaluation of alginate-gelatin hydrogel scaffolds loaded with zinc-doped hydroxyapatite and 5-fluorouracil. *Int. J. Biol. Macromol.* **2023**, *237*, 124147.

[132] Xiao, W. W.; Chen, W. L.; Wang, Y. G.; Zhang, C.; Zhang, X. C.; Zhang, S. Q.; Wu, W. Recombinant DTβ4-inspired porous 3D vascular graft enhanced antithrombogenicity and recruited circulating $CD93^{+}$/$CD34^{+}$ cells for endothelialization. *Sci. Adv.* **2022**, *8*, eabn1958.

[133] Sarkar, N.; Zhao, J. T.; Zhang, N. Y.; Horenberg, A. L.; Grayson, W. L. 3D printed O_2-generating scaffolds enhance osteoprogenitor- and type H vessel recruitment during bone healing. *Acta Biomater.* **2024**, *185*, 126–143.

[134] Su, R. G. G.; Ai, Y. J.; Wang, J. Y.; Wu, L.; Sun, H.; Ding, M. Y.; Xie, R. X.; Liang, Q. L. Engineered microfibers for tissue engineering. *ACS Appl. Bio Mater.* **2024**, *7*, 5823–5840.

[135] You, J. Q.; Li, Y. Y.; Wang, C.; Lv, H. X.; Zhai, S. B.; Liu, M. X.; Liu, X. Y.; Sezhen, Q.; Zhang, L.; Zhang, Y. D. et al. Mild thermotherapy-assisted GelMA/HA/MPDA@Roxadustat 3D‐printed scaffolds with combined angiogenesis‐osteogenesis functions for bone regeneration. *Adv. Healthcare Mater.* **2024**, *13*, 2400545.

[136] Han, Y. H.; Qin, X. Y.; Lin, W. S.; Wang, C.; Yin, X. Y.; Wu, J. X.; Chen, Y.; Chen, X. J.; Chen, T. K. Microneedle-based approaches for skin disease treatment. *Nano-Micro Lett.* **2025**, *17*, 132.

[137] Chen, Y. W.; Zou, Z. F.; Fu, T.; Li, Z.; Zhang, Z. J.; Zhu, M.; Gao, Q.; Wu, S. F.; Fu, G. S.; He, Y. et al. 3D printed grafts with gradient structures for organized vascular regeneration. *Int. J. Extrem. Manuf.* **2024**, *6*, 035503.

[138] Majrashi, M.; Kotowska, A.; Scurr, D.; Hicks, J. M.; Ghaemmaghami, A.; Yang, J. Sustained release of dexamethasone from 3D-printed scaffolds modulates macrophage activation and enhances osteogenic differentiation. *ACS Appl. Mater. Interfaces* **2023**, *15*, 56623–56638.

[139] Yang, Y. P.; Yao, Z. Y.; Sun, Y. Y.; Nie, Y. Y.; Zhang, Y. C.; Li, Z. Y.; Luo, Z. H.; Zhang, W. J.; Wang, X.; Du, Y. H. et al. 3D-printed manganese dioxide incorporated scaffold promotes osteogenic-angiogenic coupling for refractory bone defect by remodeling osteo-regenerative microenvironment. *Bioact. Mater.* **2025**, *44*, 354–370

[140] Bhat, B.; Pahari, S.; Kwon, J. S. I.; Akbulut, M. E. S. Stimuli-responsive viscosity modifiers. *Adv. Colloid Interface Sci.* **2023**, *321*, 103025.

[141] Oyunbaatar, N. E.; Kim, D. S.; Prasad, G.; Jeong, Y. J.; Lee, D. W. Self-rollable polymer stent integrated with wireless pressure sensor for real-time monitoring of cardiovascular pressure. *Sens. Actuators A: Phys.* **2022**, *346*, 113869.

[142] Carvalho, B. G.; Nakayama, A.; Miwa, H.; Han, S. W.; De La Torre, L. G.; Di Carlo, D.; Lee, J.; Kim, H. J.; Khademhosseini, A.; De Barros, N. R. Gelatin methacryloyl granular scaffolds for localized mRNA delivery. *Aggregate* **2024**, *5*, e464.

[143] Sun, J. R.; Gong, Y. P.; Xu, M. L.; Chen, H. P.; Shao, H. F.; Zhou, R. G. Coaxial 3D bioprinting process research and performance tests on vascular scaffolds. *Micromachines* **2024**, *15*, 463.

[144] Kwon, K.; Kim, J. U.; Won, S. M.; Zhao, J. Z.; Avila, R.; Wang, H. L.; Chun, K. S.; Jang, H.; Lee, K. H.; Kim, J. H. et al. A battery-less wireless implant for the continuous monitoring of vascular pressure, flow rate and temperature. *Nat. Biomed. Eng.* **2023**, *7*, 1215–1228.

[145] Glover, K.; Mathew, E.; Pitzanti, G.; Magee, E.; Lamprou, D. A. 3D bioprinted scaffolds for diabetic wound-healing applications. *Drug Deliv. Transl. Res.* **2023**, *13*, 2096–2109.

[146] Zou, Z. J.; Li, H.; Xu, G.; Hu, Y. X.; Zhang, W. G.; Tian, K. Current knowledge and future perspectives of exosomes as nanocarriers in diagnosis and treatment of diseases. *IJN* **2023**, *18*, 4751–4778.

[147] dos Santos, D. M.; Moon, J. I.; Kim, D. S.; Bassous, N. J.; Marangon, C. A.; Campana-Filho, S. P.; Correa, D. S.; Kang, M. H.; Kim, W. J.; Shin, S. R. Hierarchical chitin nanocrystal-based 3D printed dual-layer membranes hydrogels: A dual drug delivery nano-platform for periodontal tissue regeneration. *ACS Nano* **2024**, *18*, 24182–24203.

[148] Shen, Y. H.; Pan, Y. J.; Liang, F. B.; Song, J. H.; Yu, X.; Cui, J.; Cai, G. F.; El-Newehy, M.; Abdulhameed, M. M.; Gu, H. B. et al. Development of 3D printed electrospun vascular graft loaded with tetramethylpyrazine for reducing thrombosis and restraining aneurysmal dilatation. *Burns Trauma* **2024**, *12*, tkae008.

[149] Wang, C. J.; Yang, Y.; Ji, J. Y.; Fang, Y. C.; Ouyang, L. L.; Zhang, L.; Sun, W. Dd3D-printed bioresorbable stent coated with dipyridamole-loaded nanofiber for restenosis prevention and endothelialization. *Int. J. Biostat.* **2022**, *8*, 543.

[150] Kabirian, F.; Baatsen, P.; Smet, M.; Shavandi, A.; Mela, P.; Heying, R. Carbon nanotubes as a nitric oxide nano-reservoir improved the controlled release profile in 3D printed biodegradable vascular grafts. *Sci. Rep.* **2023**, *13*, 4662.

[151] Matsumoto, T.; Yoshino, S.; Furuyama, T.; Morisaki, K.; Nakano, K.; Koga, J. I.; Maehara, Y.; Komori, K.; Mori, M.; Egashira, K. Pitavastatin-incorporated nanoparticles for chronic limb threatening ischemia: A phase I/IIa clinical trial. *JAT* **2022**, *29*, 731–746.

[152] Feng, H.; Wang, X. B.; Liu, M. Y.; Liu, B.; Chen, Z.; Chen, X. M. First-in-human implantation of a 3D-printing fully bioresorbable drug eluting stent for treatment of superficial femoral artery disease. *Ann. Vasc. Surg. - Brief Rep. Innovations* **2024**, *4*, 100299.

[153] Joshi, M.; Melo, D. P.; Ouyang, D.; Slomka, P. J.; Williams, M. C.; Dey, D. Current and future applications of artificial intelligence in cardiac CT. *Curr. Cardiol. Rep.* **2023**, *25*, 109–117.

[154] Nurmohamed, N. S.; Min, J. K.; Anthopolos, R.; Reynolds, H. R.; Earls, J. P.; Crabtree, T.; Mancini, G. B. J.; Leipsic, J.; Budoff, M. J.; Hague, C. J. et al. Atherosclerosis quantification and cardiovascular risk: The ISCHEMIA trial. *Eur. Heart J.* **2024**, *45*, 3735–3747.

[155] Ihdayhid, A. R.; Tzimas, G.; Peterson, K.; Ng, N.; Mirza, S.; Maehara, A.; Safian, R. D. Diagnostic performance of AI-enabled plaque quantification from coronary CT angiography compared with intravascular ultrasound. *Radiol.: Cardiothorac. Imaging* **2024**, *6*, e230312.

[156] Albertini, J. N.; Derycke, L.; Millon, A.; Soler, R. Digital twin and artificial intelligence technologies for predictive planning of endovascular procedures. *Semin. Vasc. Surg.* **2024**, *37*, 306–313.

[157] Mensah, G. A.; Fuster, V.; Murray, C. J. L.; Roth, G. A.; Mensah, G. A.; Abate, Y. H.; Abbasian, M.; Abd-Allah, F.; Abdollahi, A.; Abdollahi, M. et al. Global burden of cardiovascular diseases and risks, 1990-2022. *J. Am. College Cardiol.* **2023**, *82*, 2350–2473.

[158] Patrick, R.; Janbandhu, V.; Tallapragada, V.; Tan, S. S. M.; Mckinna, E. E.; Contreras, O.; Ghazanfar, S.; Humphreys, D. T.; Murray, N. J.; Tran, Y. T. H. et al. Integration mapping of cardiac fibroblast single-cell transcriptomes elucidates cellular principles of fibrosis in diverse pathologies. *Sci. Adv.* **2024**, *10*, eadk8501.

[159] Paraskevas, K. I.; Brown, M. M.; Lal, B. K.; Myrcha, P.; Lyden, S. P.; Schneider, P. A.; Poredos, P.; Mikhailidis, D. P.; Secemsky, E. A.; Musialek, P. et al. Recent advances and controversial issues in the optimal management of asymptomatic carotid stenosis. *J. Vasc. Surg.* **2024**, *79*, 695–703.

[160] Gholap, A. D.; Uddin, M. J.; Faiyazuddin, M.; Omri, A.; Gowri, S.; Khalid, M. Advances in artificial intelligence for drug delivery and development: A comprehensive review. *Comput. Biol. Med.* **2024**, *178*, 108702.

[161] Udrişte, A. S.; Burduşel, A. C.; Niculescu, A. G.; Rădulescu, M.; Grumezescu, A. M. Coatings for cardiovascular stents-an up-to-date review. *IJMS* **2024**, *25*, 1078.

[162] Zhao, F.; Liu, F.; Gao, C. L.; Wang, G. Q.; Zhang, Y. F.; Yu, F.; Tian, J. W.; Tan, K.; Zhang, R. H.; Liang, K. et al. Interfacing exogenous stents with human coronary artery by self-assembled coating: Designs, functionalities and applications. *NPG Asia Mater.* **2024**, *16*, 28.

[163] Das, B. C.; Chokkalingam, P.; Masilamani, P.; Shukla, S.; Das, S. Stimuli-responsive boron-based materials in drug delivery. *IJMS* **2023**, *24*, 2757.

[164] Intravaia, J. T.; Graham, T.; Kim, H. S.; Nanda, H. S.; Kumbar, S. G.; Nukavarapu, S. P. Smart orthopedic biomaterials and implants. *Curr. Opin. Biomed. Eng.* **2023**, *25*, 100439.

[165] Antonini, L.; Poletti, G.; Pennati, G.; Petrini, L. A review on the use of finite element simulations for structural analyses of coronary stenting: What can we do nowadays and what do we need to move forward. *Eur. J. Mech. - A/Solids* **2023**, *101*, 105071.

[166] Zhu, Q. J.; Chen, Z. Z.; Wang, D.; Jiao, X. L.; Luan, Y.; Wang, M.; Luo, R. F.; Wang, Y. B.; Fu, G. S.; Wang, Y. N. et al. Microenvironment-responsive coating for vascular stents to regulate coagulation-inflammation interaction and promote vascular recovery. *Bioact. Mater.* **2025**, *48*, 443–457.

[167] Thangaraj, P. M.; Benson, S. H.; Oikonomou, E. K.; Asselbergs, F. W.; Khera, R. Cardiovascular care with digital twin technology in the era of generative artificial intelligence. *Eur. Heart J.* **2024**, *45*, 4808–4821.

[168] Han, N.; Wang, J. T.; Ma, Y. R.; Ma, L. Y.; Zheng, Y.; Fan, F. X.; Wu, C.; Yue, S. H.; Li, J.; Liang, J. et al. The hemodynamic and geometric characteristics of carotid artery atherosclerotic plaque formation. *Quant. Imaging Med. Surg.* **2024**, *14*, 4348–4361.

[169] Scicolone, R.; Vacca, S.; Pisu, F.; Benson, J. C.; Nardi, V.; Lanzino, G.; Suri, J. S.; Saba, L. Radiomics and artificial intelligence: General notions and applications in the carotid vulnerable plaque. *Eur. J. Radiol.* **2024**, *176*, 111497.

[170] Dong, W. Y.; Jiang, H. C.; Li, Y.; Lv, L.; Gong, Y. X.; Li, B.; Wang, H. J.; Zeng, H. S. Interpretable machine learning analysis of immunoinflammatory biomarkers for predicting CHD among NAFLD patients. *Cardiovasc. Diabetol.* **2025**, *24*, 263.

[171] Singh, A.; Miller, R. J. H.; Otaki, Y.; Kavanagh, P.; Hauser, M. T.; Tzolos, E.; Kwiecinski, J.; Van Kriekinge, S.; Wei, C. C.; Sharir, T. et al. Direct risk assessment from myocardial perfusion imaging using explainable deep learning. *JACC: Cardiovasc. Imaging* **2023**, *16*, 209–220.

[172] Jain, S. S.; Elias, P.; Poterucha, T.; Randazzo, M.; Lopez Jimenez, F.; Khera, R.; Perez, M.; Ouyang, D.; Pirruccello, J.; Salerno, M. et al. Artificial intelligence in cardiovascular care-part 2: Applications. *J. Am. College Cardiol.* **2024**, *83*, 2487–2496.

[173] Le, E. P. V.; Wong, M. Y. Z.; Rundo, L.; Tarkin, J. M.; Evans, N. R.; Weir-McCall, J. R.; Chowdhury, M. M.; Coughlin, P. A.; Pavey, H.; Zaccagna, F. et al. Using machine learning to predict carotid artery symptoms from CT angiography: A radiomics and deep learning approach. *Eur. J. Radiol. Open* **2024**, *13*, 100594.

[174] Wang, C. Y.; Liu, S. R.; Yang, H.; Guo, J. L.; Wu, Y. X.; Liu, J. L. Ethical considerations of using ChatGPT in health care. *J. Med. Internet Res.* **2023**, *25*, e48009.

[175] Preiksaitis, C.; Ashenburg, N.; Bunney, G.; Chu, A.; Kabeer, R.; Riley, F.; Ribeira, R.; Rose, C. The role of large language models in transforming emergency medicine: Scoping review. *JMIR Med. Inform.* **2024**, *12*, e53787.

[176] Gottardelli, B.; Gatta, R.; Nucciarelli, L.; Tudor, A.; Tavazzi, E.; Vallati, M.; Orini, S.; Di Giorgi, N.; Damiani, A. GEN-RWD sandbox: Bridging the gap between hospital data privacy and external research insights with distributed analytics. *BMC Med. Inform. Decis. Mak.* **2024**, *24*, 170.

[177] Mao, Y.; Ren, J.; Yang, L. F. Advances of nanomedicine in treatment of atherosclerosis and thrombosis. *Environ. Res.* **2023**, *238*, 116637.

[178] Nakano, K.; Matoba, T.; Koga, J. I.; Kashihara, Y.; Fukae, M.; Ieiri, I.; Shiramoto, M.; Irie, S.; Kishimoto, J.; Todaka, K. et al. Safety, tolerability, and pharmacokinetics of NK-104-NP. *Int. Heart J.* **2018**, *59*, 1015–1025.

[179] Tian, J. Q.; Han, Z. P.; Song, D. D.; Peng, Y. J.; Xiong, M.; Chen, Z.; Duan, S. Y.; Zhang, L. Engineered exosome for drug delivery: Recent development and clinical applications. *Int. J. Nanomed.* **2023**, *18*, 7923–7940.

[180] Alzoubi, L.; Aljabali, A. A. A.; Tambuwala, M. M. Empowering precision medicine: The impact of 3D printing on personalized therapeutic. *AAPS PharmSciTech* **2023**, *24*, 228.

[181] Sun, Z. H.; Jansen, S. Personalized 3D printed coronary models in coronary stenting. *Quant. Imaging Med. Surg.* **2019**, *9*, 1356–1367.

[182] Wang, C. T.; Zhang, L.; Qin, T.; Xi, Z. L.; Sun, L.; Wu, H. W.; Li, D. M. 3D printing in adult cardiovascular surgery and interventions: A systematic review. *J. Thorac. Dis.* **2020**, *12*, 3227–3237.

[183] Jiang, H.; Ye, L. S.; Zhang, Y. H.; Liu, C. Q.; Chen, L. X.; Gao, Y.; Yang, J. C.; Hu, B. Current status and future trends of biodegradable stents for esophageal stenosis: A literature review. *Chin. Med. J.* **2024**, *137*, 2638–2640.

[184] Khan, M. A.; Khan, N.; Ullah, M.; Hamayun, S.; Makhmudov, N. I.; Mbbs, R.; Safdar, M.; Bibi, A.; Wahab, A.; Naeem, M. et al. 3D printing technology and its revolutionary role in stent implementation in cardiovascular disease. *Curr. Probl. Cardiol.* **2024**, *49*, 102568.

[185] Lin, A.; Manral, N.; McElhinney, P.; Killekar, A.; Matsumoto, H.; Kwiecinski, J.; Pieszko, K.; Razipour, A.; Grodecki, K.; Park, C. et al. Deep learning-enabled coronary CT angiography for plaque and stenosis quantification and cardiac risk prediction: An international multicentre study. *Lancet Digital Health* **2022**, *4*, e256–e265.

[186] Nurmohamed, N. S.; van Rosendael, A. R.; Danad, I.; Ngo-Metzger, Q.; Taub, P. R.; Ray, K. K.; Figtree, G.; Bonaca, M. P.; Hsia, J.; Rodriguez, F. et al. Atherosclerosis evaluation and cardiovascular risk estimation using coronary computed tomography angiography. *Eur. Heart J.* **2024**, *45*, 1783–1800.

[187] Mastrodicasa, D.; van Assen, M.; Huisman, M.; Leiner, T.; Williamson, E. E.; Nicol, E. D.; Allen, B. D.; Saba, L.; Vliegenthart, R.; Hanneman, K. Use of AI in cardiac CT and MRI: A scientific statement from the ESCR, EuSoMII, NASCI, SCCT, SCMR, SIIM, and RSNA. *Radiology* **2025**, *314*, e240516.

[188] Liu, Y.; Ma, S. C.; Li, F.; Ding, H. S.; Zhang, Q.; Yu, F. F.; Zhang, H. P.; Hao, Y. J.; Liu, B.; Jiang, Y. D. Biomimetic nanocomplexes loading with evolocumab and curcumin for synergistic anti-atherosclerosis therapy in ApoE$^{-/-}$ mice. *J. Nanobiotechnol.* **2025**, *23*, 412.

[189] Cesaro, A.; Acerbo, V.; Indolfi, C.; Filardi, P. P.; Calabrò, P. The clinical relevance of the reversal of coronary atherosclerotic plaque. *Eur. J. Intern. Med.* **2024**, *129*, 16–24.

[190] Zhao, Y.; Chen, J. Q.; Andreatta, M.; Feng, B.; Xie, Y. Q.; Wenes, M.; Wang, Y.; Gao, M.; Hu, X. M.; Romero, P. et al. IL-10-expressing CAR T cells resist dysfunction and mediate durable clearance of solid tumors and metastases. *Nat. Biotechnol.* **2024**, *42*, 1693–1704.

[191] Verma, N.; Setia, A.; Mehata, A. K.; Randhave, N.; Badgujar, P.; Malik, A. K.; Muthu, M. S. Recent advancement of indocyanine green based nanotheranostics for imaging and therapy of coronary atherosclerosis. *Mol. Pharm.* **2024**, *21*, 4804–4826.

[192] Bartusik-Aebisher, D.; Podgórski, R.; Serafin, I.; Aebisher, D. Targeted and biomimetic nanoparticles for atherosclerosis therapy: A review of emerging strategies. *Biomedicines* **2025**, *13*, 1720.

[193] Szebeni, J.; Storm, G.; Ljubimova, J. Y.; Castells, M.; Phillips, E. J.; Turjeman, K.; Barenholz, Y.; Crommelin, D. J. A.; Dobrovolskaia, M. A. Applying lessons learned from nanomedicines to understand rare hypersensitivity reactions to mRNA-based SARS-CoV-2 vaccines. *Nat. Nanotechnol.* **2022**, *17*, 337–346.

[194] Mehta, G.; Ferreira, V. P.; Skerka, C.; Zipfel, P. F.; Banda, N. K. New insights into disease-specific absence of complement factor H related protein C in mouse models of spontaneous autoimmune diseases. *Mol. Immunol.* **2014**, *62*, 235–248.

[195] Chen, B. M.; Cheng, T. L.; Roffler, S. R. Polyethylene glycol immunogenicity: Theoretical, clinical, and practical aspects of anti-polyethylene glycol antibodies. *ACS Nano* **2021**, *15*, 14022–14048.

[196] Salih, A.; Boscolo Galazzo, I.; Gkontra, P.; Lee, A. M.; Lekadir, K.; Raisi-Estabragh, Z.; Petersen, S. E. Explainable artificial intelligence and cardiac imaging: Toward more interpretable models. *Circ.: Cardiovasc. Imaging* **2023**, *16*, e014519.

[197] Corral-Acero, J.; Margara, F.; Marciniak, M.; Rodero, C.; Loncaric, F.; Feng, Y. J.; Gilbert, A.; Fernandes, J. F.; Bukhari, H. A.; Wajdan, A. et al. The 'Digital Twin' to enable the vision of precision cardiology. *Eur. Heart J.* **2020**, *41*, 4556–4564.